Factors Contributing to Volcano Lateral Collapse

# Factors contributing to volcano lateral collapse

Matteo Roverato[1,2], Federico Di Traglia[3], Jonathan Procter[4], Engielle Paguican[5,6], Anja Dufresne[7]

1- School of Earth Science, Energy and Environment, Yachay Tech University, Urcuqui, Ecuador
2- Department of Earth Sciences, University of Geneva, Switzerland
3- Dipartimento di Scienze della Terra, Università degli Studi di Firenze, Firenze, Italy
4- School of Agriculture and Environment, Massey University, Private Bag 11 222, Palmerston North, New Zealand
5- School of Geography, Environment and Earth Science, University of the South Pacific, Laucala Campus, Suva, Fiji
6- College of Engineering and Geosciences, Caraga State University, Ampayon, Butuan City, Philippines
7- Engineering Geology and Hydrogeology, RWTH-Aachen University, Aachen, Germany

**Abstract**

Many factors can lead to volcano lateral collapse, which can produce devastating debris avalanches that travel up to several tens to over 100 km and cover hundreds to more than a thousand km$^2$ with debris. Volcanic lateral collapses are severe hazards because of their destructive power and size, and sudden onset. Although their frequency of occurrence is not as high as those of smaller volcanic mass movements, such as rock falls and lahars, globally large collapses ≥0.1 km$^3$ have occurred at least five times per century over the last 500 years. A large variety of destabilizing factors such as over-steepened slopes, magma intrusions, hydrothermal activity, climate fluctuations, deformation of the basement, and faulting can create the conditions for volcano collapse. Once a volcano reaches its critical point, a mechanism is necessary to trigger the failure event. We present the state-of-the-art of the knowledge acquired in the last few decades concerning the causes of large-scale volcanic failures to better understand the triggers, preparatory factors, and timing of volcano lateral collapse.

**Keywords**: volcanic lateral collapse; debris avalanche; instability factors; triggering mechanisms

## 1 - Introduction

Large long-lived composite volcanoes are positive topographic structures characterized mainly by constructive phases. The stability of the edifice is primarily controlled by the characteristics of the outer slope, which, when it reaches a critical configuration, can become unstable. Edifice failure may also be triggered by external processes even before it reaches its critical configuration. Slope instability in volcanoes typically results in a structural failure leading to lateral collapse. Volcano flank movement can be classified as: i) persistent flank motion, typically deep-seated, steady-state movement of large sectors of a volcano edifice due to gravity; ii) transient flank motion (i.e. flank "unrest"), considered the precursor to catastrophic collapses, associated with intrusive processes, co-eruptive deformation, seismic shaking; or iii) surficial slope motion, or shallow motion such as material erosion and remobilization of volcaniclastic and lava deposits (Schaefer et al. 2019). Edifice collapses are not restricted to stratovolcanoes, but have occurred on all types of volcanoes (dome complexes, shield volcanoes, calderas and even within monogenetic fields) (Dufresne et al. 2020; this volume) and may happen in all geodynamic contexts (Ui 1983; Siebert 1984; McGuire 1996; Voight and Elsworth 1997; Voight 2000; Shea and Van Wyk de Vries 2010; Van Wyk de Vries and Davies 2015).

Such volcano sector collapses leave behind a scar that could be of a caldera size (kilometers across) and shape (Siebert, 1984; McGuire 2006). This might explain why, before the 1980 Mount St. Helens event, many wide depressions hosted in volcanic summits were considered calderas (Siebert and Roverato 2020 - this volume), which form by vertical subsidence along ring faults due to eruptive events, rather than by a lateral collapse. This erroneous interpretation is understandable because horseshoe-shaped scar can be partly obliterated by volcano regrowth covering the failure area with new eruption deposits. Belousov et al. (1999) wrote: "Evaluation of known cases of large-scale failures on volcanoes throughout the world shows that failure can occur, given the right combination of circumstances, at almost any reasonably high volcanic edifice". It appears that this behavior is ubiquitous, with evidence for volcanic failures both within the geological record and at many currently active volcanoes. For example, Francis (1994) wrote that 75% of Andean volcanic edifices, with heights greater than 2,500 m, have experienced at least one sector collapse, while in Indonesia, most volcanoes with heights greater than 2,000 m have suffered the same fate (MacLeod 1989). Inokuchi (1988) reported that over 100 volcanic debris avalanche deposits (VDADs) have been identified around Japanese Quaternary

68 volcanoes. Volcanic collapses, and their associated VDAs, are severe potential hazards not
69 only because of their destructive power and size but, as stressed by Siebert and Roverato
70 2020 – this volume), because volcanic edifice failures ≥0.1 $km^3$ have occurred at least five
71 times per century over the last 500 years. Augustine volcano (Alaska, USA) has repeatedly
72 collapsed, once every 150-200 years during the past 2,000 years (Begét and Kienle, 1992),
73 although those were at relatively "small" volumes (< 0.25 $km^3$). Mount Taranaki (New
74 Zealand) shows a similar pattern of growth and collapse with 14 VDADs over its 120,000
75 years evolution with a regular 16,000 years return period (Zernack et al. 2012). Colima
76 volcano collapsed at least nine times during the last 20,000 years (Capra et al. 2002). This
77 frequency and cyclic behavior should not be underestimated for hazard assessment.
78 The study of this type of phenomenon strengthened after the collapse and eruption
79 of Mount St. Helens volcano (USA) on 18 May 1980. This event represents the only case
80 where lateral collapse of the volcanic edifice has been observed directly (Lipman and
81 Mullineaux 1981). Although the eruption of Mount St. Helens represented an event of great
82 importance for the understanding of such phenomenon linked to the collapse of a volcanic
83 edifice, the factors that prepare and trigger these events are not simple, but can be multiple
84 and combined. The effects of a volcanic lateral collapse are usually of great magnitude.
85 Mass movement on volcanic slopes can occur at different scales, which can span from
86 relatively minor rock falls consisting of a few hundred to a few thousand cubic meters of
87 material up to the giant landslides that may involve materials more than 1,000 $km^3$
88 (McGuire 1996, 2003). Events involving small volumes of material may occur with time
89 intervals of weeks or months, whereas larger events are having frequencies of 10s to 100s
90 of thousands of years (Schaefer et al. 2019). The large volumes observed in many volcanic
91 debris avalanches involve the collapse of part of a volcanic edifice and this can in turn
92 influence the runout of a VDAD. These destructive flows can travel at high velocities, cover
93 large areas, overcome topographical barriers and modify the topography in seconds.
94 Generally, these deposits could preserve evidence of the cause of the instability, but it is
95 often difficult to determine the triggering mechanism. Volcanic lateral collapses can be
96 caused by a wide variety of destabilizing factors such as over-steepened slopes, increasing
97 fluid pore pressures (consequence of several combined factors), magma intrusions,
98 hydrothermal alteration, climate fluctuations, deformation of the basement, cataclysmic
99 eruptions, among others (Table 1). It is important to identify the differences between those

factors that define the degree of instability of a volcanic edifice from those mechanisms that trigger the collapse. Indeed, the mechanism that triggers a sector collapse could be independent of the causes that prepare its instability. For example, the tectonic setting of a volcano may influence the direction of the collapse and prolonged hydrothermal alteration can deeply weaken the edifice, but the collapse itself could be triggered by an eruption or an earthquake.

Table 1

Sector collapses can cause tsunamis or lahars increasing the areas and population at risk. In 2018, tsunamigenic lateral collapse of Anak Krakatau, Indonesia (Williams et al. 2019) and lateral collapse of Kilauea, US (Chen et al. 2019) and Etna, Italy (Bonforte et al. 2019) occurred, with resulting loss of life and property. It is therefore important to understand the instability factors and triggers of volcano lateral collapse since that knowledge can provide very important precursory information that can directly improve hazard warnings (Capra 2006).

## 2 - Instability factors

A wide range of factors may contribute to the instability of a volcanic edifice, and some volcanoes are more prone to lateral failure than others, depending on their structure and the environment in which they form (McGuire 2003). Large-scale structural instability is invariably confined to major composite volcanoes, located either on continental (e.g. Shiveluch in Russia, Taranaki in New Zealand, and Colima in Mexico) or oceanic (e.g. Teide in Canary Islands - Spain, and Piton de la Fournaise on Reunion Island) crust. Destabilization of a volcanic edifice may take thousands or tens of thousands of years, or it may be achieved in only a few months (McGuire 2003). One well-known example of short-lived destabilization-to-collapse event is the Mount St. Helens collapse, where a cryptodome intruded into the edifice only few months before the collapse. That is in contrast to slow, incremental and progressive factors, such as long-term hydrothermal alteration, or long-lasting deformation that can occur individually or often act together as cumulative effects of many small events. Below, we describe the instability factors that favor the weakening of a volcanic edifice and promote sector collapses.

## 2.1 Basement, tectonics, and faults

Volcanism is linked to tectonically active regions, whether extensional, compressional or along transcurrent faulting, in both transcompressional and transtensional regimes (Tibaldi et al. 2005). Tectonic faults propagate from the substrate and into the volcano edifice, where their geometry and kinematics become more complex. A close relationship exists between fault movement and the stability of the overlying volcanic edifice: basement faults affect volcanoes (Francis and Self 1987; Carracedo 1994; Tibaldi 1995) and vice versa (van Wyk de Vries and Merle 1996; van Wyk de Vries 1998). Volcano edifice morphology, including collapse directions and fracture planes used as pathways for magma, respond to regional stress fields in complex ways (Delaney et al. 1986). Preferential directions of progressive flank destabilization depend not only upon the orientation, kinematics, and dip and inclination of basement faults (Tibaldi et al. 2005), but also on the position of the fault within the edifice (Norini et al. 2008; Wooller et al. 2009; Norini et al. 2020). Once volcanic failure occurs, the collapse depression and the new geometry of the volcanic edifice strongly influence the location and configuration of new craters and dykes.

Nakamura (1977) suggested that cone elongation, strike of dikes and fractures, and alignment of flank vents occur parallel to the regional maximum compressive stress direction (σHmax) (Figurea). Moriya (1980) suggested that the elongated growth of volcanic flanks parallel to dike emplacement, steeper slopes normal to the elongation direction of volcanoes, and the dilatational effect of dike intrusion all promote failure perpendicular to σHmax, as was observed at 30 Japanese volcanoes. The higher percentage of volcanoes with parallel dike swarms that formed amphitheater-like scars relative to volcanoes without a dominant direction of dike orientation indicates that dike swarms that develop parallel to σHmax play an important role in volcanic lateral collapse (Siebert 1984). Francis and Wells (1988) suggested a model of failure scar opening perpendicular to the strike of normal faults and σHmax (Figureb).

These models, however, are not consistent with the alignment of volcanoes, dikes, flank vents, and collapse directions in Indonesia, where they tend to be at a high angle to σHmax as determined from fault-fold structures in the region (Bahar and Girod 1983). An examination of 39 Japanese volcanoes revealed failure scar openings at an acute angle relative to σHmax (Ui et al. 1986). The same is true for the 28 examples of breached cones in the Central Andes (Figurec) (Francis and Wells 1988).

Figure 1

The inconsistencies in these studies led to the idea that the opening direction may not be influenced by the regional tectonic field, but may be controlled by temporal and local stress fields within the volcanic edifice or the different geodynamic settings where volcanoes are located (Ui et al. 1986).

In a study of 1,315 Quaternary volcanoes in different structural settings, Tibaldi (1995) established that failure scar breaching perpendicular to fault strike is prevalent in extensional regions, and collapses are usually in the direction of the downthrown block (Vidal and Merle 2000). This is consistent with the model of Moriya (1980) and Siebert (1984), where plate-shaped conduits and dikes could propagate through extensional faults and thereby promote collapse perpendicular to the regional σHmax. Also, in extensional regimes, the regional stress field produces brittle discontinuities that crosscut the edifice by forming rift zones, used as a pathway for the magma to reach the surface. This feeds dyke swarms in a preferred orientation, which then displace the volcano flanks and may induce lateral collapse of the edifice (Elsworth and Voight 1996; Tibaldi 1996).

In contrast to extensional regions, breaching in volcanoes along transcurrent faults or transtensional tectonics is at an acute angle relative to σHmax (Tibaldi, 1995; Norini et al., 2008). This is true for the volcanoes in Southwest and Southeast Luzon, Philippines including Iriga (Figure 1d; Lagmay et al. 2000; Lagmay and Valdivia 2006; Paguican et al. 2012), as well as Mount St. Helens, USA. Lateral collapses in transtensional tectonic regions underlain by normal faults are more diffused compared to transcompressional and reverse tectonic regions due to tilting and topographic offsets within the basement (Tibaldi 2005). Analogue experiment by Lagmay et al. (2000) and Norini and Lagmay (2005) showed that edifices on top of strike-slip faults form a pair of sigmoids composed of one reverse and one normal fault on the surface, and a flower structure in the interior of the edifice. Two destabilized regions characterized by bulging and landsliding are created on the flanks between the traces of the sigmoidal faults. Sigmoidal summit depressions, fractures, and faults developed within the edifice create space for subsequent magma intrusion, thus causing further instability (van Wyk de Vries and Merle 1996).

195 The variety of fault types and geometries has a general tendency to produce regions
196 of instability parallel to fault strike, irrespective of the fault motion. Analogue experiments
197 by Wooller et al. (2009) showed that in oblique-slip faulting, the instability is always on the
198 downthrown side, and usually in the volcano sector facing the strike-slip sense of motion
199 (Figure 2). The location, type, and magnitude of instability of the edifice changes with the
200 position of the fault beneath the analogue volcano. The further the fault is from the central
201 axis, the larger the destabilized sector. Also, with greater fault offset from the central axis,
202 larger unstable volumes are generated. Such failures are perpendicular to the strike of the
203 underlying fault.
204 These models may not work in volcanoes where an underlying sloping substrate or
205 gravitational spreading have a stronger influence on the collapse direction (van Wyk de
206 Vries and Merle 1996).
207
208 Figure 2
209
210 **2.2 Sloping substrate and gravitational spreading**
211 Many volcanoes grow on sloping ground, and some of them tend to slide downhill
212 and collapse catastrophically on the downslope side (Vallance et al. 1995; Carrasco-Núñez et
213 al. 2006; Murray et al. 2018). Many large stratovolcanoes worldwide are directly in contact
214 with thick sedimentary or igneous sequences that have been affected by different
215 compressional and extensional processes depending on the geotectonic evolution of the
216 area (e.g. the Andean mountain range). These sequences often appear tilted, showing a
217 certain grade of dipping and generating a strength anisotropy. In northern Chile, for
218 example, widespread ignimbrite sheets and thick ductile Cenozoic sedimentary deposits dip
219 toward the west into the Salar de Atacama basin with an angle of 5° (Wooller et al. 2004).
220 The Tumisa volcanic complex, located northward in the same region, is underlain by several
221 hundred meters of salt-rich lake sediments, ignimbrites and evaporite deposits, which
222 together form a westward-dipping ductile package (Kuhn 2002). According to Wooller et al.
223 (2004), the entire Tumisa volcanic complex has undergone a downslope sliding toward the
224 same western direction. Analogue experiments presented by these authors demonstrate

that volcano spreading is highly dependent on substrata dip and spreading occurs even at very small substrata tilt (< 1°).

Many other Central Andean volcanoes experienced slope collapses that left horseshoe-shaped scars oriented toward the direction of the regional slope (Francis and Wells 1988). Vallance et al. (1995) noted a similar pattern with Guatemalan volcanoes, which failed preferentially trenchward to the southwest in the direction of regional slope of the Guatemalan Highlands. At the eastern end of the Mexican Volcanic Belt, the Cofre de Perote-Citlatépetl range is constructed at the margin of the Altiplano. The basement drops dramatically to the Caribbean coastal plain, and all collapse events have been in that direction (Carrasco-Núñez et al. 2006). In Central America, Siebert et al. (2006) noted that with volcanoes at the far ends of the arc, failures tended to occur preferentially perpendicular to the trend of the arc and in a direction toward the Central-American trench. In contrast, volcanoes in El Salvador and Nicaragua in the center of the arc, where the basement topographic effect is less pronounced, have more variable failure directions. This is even more pronounced at an isolated island volcano like Augustine in Alaska, without regional topographic gradients, where failures occurred radially in all directions (Begét and Kienle 1992).

The same behavior occurs at volcanoes in Indonesia that are located on dipping ductile substrata and have undergone volcano spreading, or at the volcanoes belonging to the Lesser Antilles, in the Caribbean Sea. Deplus et al. (2001) report that the volcanoes are situated on westward-dipping substrata related to the Tertiary Caribbean arc, the same orientation in all major collapses of the region.

Numerous studies (Merle and Borgia 1996; Lundgren et al. 2004; Bonforte et al. 2011; Murray et al. 2018) reveal that the eastern and southern flanks of Mt. Etna are sliding eastward towards the Mediterranean Sea, affected by the slope and lithology of the basement, with zones of differential velocities forming several fault-bounded blocks. It is not coincidental that the “Valle del Bove” scar is oriented in the same direction as Mt. Etna creeps. Lateral collapses might also occur for those volcanoes located on steeper dip slopes, compared with low-angle dip basement mentioned above. Due to the migration of an eruptive vent, a consequence of various factors (e.g. changes in the plate subduction angle, variation in the tectonic setting, migration of the magma chamber, among others), a volcano might grow on the flank of an older volcanic edifice with slopes angles > 20-25°. A

257 good example is the Fuego de Colima volcano (Fig. 3), which is located on the southern flank
258 of the older and inactive Nevado de Colima volcano. Whilst the direction of the sector
259 collapses of the Nevado de Colima volcano has been controlled by the Colima Rift
260 confinement (Norini et al. 2019), the inclination of the southward dipping Nevado de Colima
261 flank appears to be the main topographic constraint generating the instability of the Fuego
262 de Colima edifice (Norini et al. 2010; Roverato et al. 2011; Norini et al. 2019).
263
264 Figure 3
265
266 At a lower scale, on 16 November 2006 a lateral collapse affected the unstable
267 eastern slope of the steep South-East Crater (SEC) of Mount Etna, built on one side of the
268 steep central craters of the volcano (Norini et al. 2009). The collapse was triggered by
269 erosion of loose, hydrothermally altered material of the steep south-east sector of SEC from
270 the outpour of lava and produced a landslide of 330,000 - 413,000 $m^3$ that involved both
271 lithic and juvenile material, resulting in a deposit emplaced on the eastern flank of the
272 volcano (Norini et al. 2009). Thus, the substrata dip and the steepness of volcano flanks is
273 important for volcanic edifice instability, as it can control the spreading to downslope
274 sectors and the associated sector-collapse volumes. Differential buttressing at the volcano
275 base is also a major factor controlling flank instability and is an important indication to
276 expect asymmetric activity in any volcano, like flank eruptions and deformations (Norini and
277 Acocella 2011).
278 Volcanic gravitational spreading is one of the most complex factors contributing to
279 instability that can affect a volcanic edifice. This is because numerous variables are involved
280 in the process, although the most important of those is the substratum on which the
281 volcano sits. Gravitational spreading is the result of a set of processes that translate the
282 vertical volcano load into horizontal movement, accommodated by high-angle normal faults
283 on the edifice's slopes and low-angle thrust faults at its boundaries and in the substratum.
284 In a pioneer work, van Bemmelen (1949) reported faults across volcanic edifices and
285 anticlinal ridges and low-angle thrusts along their peripheries for several Indonesian
286 volcanoes (e.g. Soropati, Lawu, Merapi, Bukittunggul, Tjereme). These volcanoes are built
287 on thick sequences of marine clays and fine-grained deposits. The deformation structures of
288 the substrata are attributed to sediment faulting beneath the volcanoes in response to

gravitational loading (Borgia et al. 2002). At Parinacota (Chile), the deformation of low-density unconsolidated fluvio-glacial and lacustrine sediments and pyroclastic basin-fill sequences in response to volcano loading is considered as the main causative factor of the ca. 8,000 years old slope collapse that produced a 6 $km^3$ VDAD (Clavero et al. 2002). Other researchers described such typical features of deformation in the substratum sediments, and it appears that they play a fundamental role in controlling the stability of a volcanic edifice and the size of the collapsed landslide. At Mombacho volcano (Nicaragua), two Holocene collapses are well described in the literature, one toward the south (El Crater) and the other to the northeast (Las Isletas) (van Wyk de Vries and Francis 1997; Shea et al. 2008; Shea and van Wyk De Vries 2010). The base of Mombacho volcano in its northeastern side is surrounded by an anticline structure, which was likely formed as Mombacho was slowly spreading outwards (Shea and van Wyk de Vries 2010). A pumice-rich substratum has also been found at the base of the Las Isletas VDAD, much further from the original in-situ ignimbrite deposit. Sedimentary sequences in the deposit indicate extrusion of the substratum, which is eventually ripped up and transported by the VDA resulting from lateral collapse. Socompa volcano, located on the southeastern margin of the Atacama basin (Chile/Argentina), suffered a dominantly westward gravitational spreading (Wooller et al. 2004). The collapse was triggered by failure of active thrust-anticlines in sediments underlying the volcano. High amounts of the substratum sediments have been found within the Socompa VDAD (van Wyk de Vries et al. 2001).

Two distinct styles of deformation are described: 1) “volcano spreading” if the volcanic edifice spreads with the substrata, and 2) “substrata extrusion” (van Wyk de Vries and Matela 1998) when the volcano and substrata are decoupled and the substrata are extruded from under the edifice. In both cases, compressional structures are produced at the base of the volcano. At Socompa volcano, the gravitational deformation has developed mainly by substrata extrusion expressed by a series of thrust anticlines (van Wyk de Vries et al. 2001). Major structures observed on the summit of other volcanoes like Etna and Kilauea (Borgia et al. 1992; Morgan et al. 2003; Urlaub et al. 2018) suggest that, at the beginning of gravitational spreading, the volcanoes present grabens and rifts on their summits. These features are also reported by Del Camp et al. (2008) for Piton de la Fournaise volcano (Reunion Island), Concepción and Maderas volcanoes (Nicaragua), Merapi volcano (Indonesia), and other Andean Chile/Bolivian volcanoes. Recent analogue models by Shea

and van Wyk de Vries (2008), Andrade and van Wyk de Vries (2010) and Paguican et al. (2012) explored the kinematics of a volcanic failure from the early stages of a sector collapse. Andrade and van Wyk de Vries (2010) reproduced in their experiments how grabens and rift-structures develop at the summit of volcanic edifices in response to the compressional forces at the base of the edifice. Furthermore, they report that most of the viscous basal layers used in the experiments had been expelled from underneath the volcano as in natural examples (van Wyk de Vries and Francis, 1997; van Wyk de Vries et al. 2001). One important insight from these experiments is that gravitational spreading stops or is reduced after a catastrophic collapse (Andrade and van Wyk de Vries 2010). This is an obvious conclusion as the volcanic loading decreases considerably after part of the edifice is removed and spread onto the surrounding landscape. Alternatively, gravitational spreading enhances catastrophic collapse only during its initial stages. When no catastrophic collapse occurs, the volcanic edifice will continue to spread progressively, gradually reducing the slope of its flanks (Andrade and van Wyk de Vries 2010; Norini et al. 2010).

### 2.3 Hydrothermal alteration

Volcanoes are actively growing and evolving systems characterized by the interaction of fluids, gases and heat that can hydrothermally alter the edifice. Hydrothermal alteration causes rock dissolution and mineral-chemical modification, it can promote high pore pressures, weaken the volcanic edifice's rocks and increase the overall clay-content. Hydrothermal alteration can occur progressively over long periods (>100 yrs), allowing deformation to develop slowly before collapse (Van Wyk de Vries et al. 2000). Each hydrothermal system develops in a unique manner depending on the rate of fluids that circulate within the volcano, their temperature, the porosity and permeability of the material forming the edifice, as well as the amount of external meteoric water infiltrating into the edifice. Consequently, each hydrothermal system has its own distinctive size, volume, chemical, and physical characteristics (Cecchi et al. 2004). Many large volcanic lateral collapses have involved hydrothermally altered rocks (Siebert 1984), which can be a useful indicator of the source of the collapse, and the slope destabilization and collapse triggering mechanisms. Examples of VDADs that display hydrothermal alteration (Figure 4) are reported in the literature and some are listed in Table 2.

Figure 4

Clay minerals from hydrothermal alteration are also found in some avalanche-induced lahar deposits at Mount Rainer, including the 3.8 $km^3$ Osceola mudflow (Vallance and Scott 1997), the 0.2 $km^3$ Round Pass mudflow, and the 0.26 $km^3$ Electron mudflow (Scott et al. 1995). The presence of hydrothermally altered rocks in these deposits suggests that this process partly weakened the edifice and likely promoted the slope collapse (Reid et al., 2001). Mount Rainier has large areas of hydrothermally altered rocks (Frank, 1995; Zimbelman, 1996; Reid el., 2001; John et al., 2008). Reid et al. (2001) noted that the alteration in highly porous rocks such as scoria and pumice is less intense and present mainly as vesicle infillings. On the other hand, the alteration is more severe in dense lavas and dikes, largely obliterating original igneous minerals and textures, and contributing to an overall reduction in rock mass strength.

Table 2

The Holocene Teteltzingo deposit, a ~2 $km^3$ clay-rich VDAD formed by the Citlaltépetl (Mexico) volcano's slope collapse, displays a high clay content in the range of 10 to 16% (Carrasco-Núñez et al., 1993). Its features suggest that it had an origin from a water-saturated hydrothermally altered edifice and that it transformed into a cohesive lahar at the very beginning of the failure event. The volume of altered rocks involved in the collapse was on the order of $10^8$ to $10^9$ $m^3$ (Carrasco-Núñez et al. 1993). Currently, the Citlaltepetl volcano is still characterized by a widespread alteration enhanced by the glacier (melted-ice circulation), including massive zones of replacement and vein fillings along numerous fractures (Zimbelman et al. 2004). Much of the replacement alteration is of acid sulfate. During vapor condensation, the $SO_2$ responsible for the alteration is present in very high concentrations, and a fluid of very low pH forms (Zimbelman et al. 2004). This acid brine reacts with the host rocks, leaching it and creating an increase in permeability. The voids left by the acid dissolution are now available to be filled by fluids such as meteoric water, which may increase the pore pressure into the volcanic edifice if sufficient water exploits the new pathways. Lopez and Williams (1993) stressed the importance of hydrothermal fluids circulation into a volcanic edifice and considered the hot spring compositions, residence times and flow path through faults of fluids to model potential collapse scenarios at Nevado

386 del Ruiz volcano (Colombia). The continual hydrothermal activity reduces the strength of the
387 rock (mainly due to clay mineral formation), and favors the more porous lithologies, which,
388 in turn, can increase pore pressures when fluids fill the voids (Day 1996; Voight and
389 Elsworth 1997; Reid 2004). Day (1996) suggests that the hydrothermal alteration is more
390 effective in the interior of volcanic edifices where higher pressures and temperatures could
391 dissolve the rocks more effectively (Frantz et al. 1981) creating high-permeability zones. On
392 the contrary, in the exterior and cooler parts of the edifice, clay minerals will precipitate
393 from the hydrothermal fluids, decreasing the permeability and promoting for example,
394 meteoric water storage. There is growing evidence that the internal fluid pressure in a
395 volcanic edifice is one of the main factors for potential instability. For example, Borselli et al.
396 (2011) report that, at Colima volcano (Mexico), the fluid pressure likely produces a local
397 reduction of shear strength along a portion or all of a potential sliding surface, promoting a
398 global reduction of the stability factor of the volcanic edifice. This idea is supported by a
399 recent resistivity tomography survey by Rosas-Carbajal et al. (2016) in which they
400 investigated the structure and dynamics of the hydrothermal system at La Soufrière volcano
401 (Guadalupe). The authors suggested that highly altered, fluid-saturated, weak zones and the
402 low basal friction of argilized detachment planes could significantly reduce the factor of
403 safety of the volcano slope. Finally, the recent study of Delmelle and Bernard (2015) showed
404 how slope instabilities, associated with hydrothermal alteration, can increase by the
405 formation of acidic crater lakes on the summits or within the flank topography of active
406 volcanoes, such as the Kawah Ijen hyperacid lake (pH< 0.5) on the flank of Merapi volcano.
407 Leakages through the flanks of the acid lake and dissolution beneath it, weakens the interior
408 of the volcano and build a substantial body of highly altered rock within the upper part of
409 the volcanic edifice that reduces its stability (Delmelle et al. 2015).
410
411 **2.4 Dikes and magma intrusions**
412 Historical volcanic lateral collapses at Bezymianny, Kamchatka in 1957, Mount St.
413 Helens in 1980, and Soufrière Hills, Montserrat in 1997, all generated large eruptions with
414 associated lateral blasts caused by large-scale deformation and steepening of flanks prior to
415 failure (Gorshkov and Bogoyavkenskaya 1965; Gorshkov 1959; Voight et al. 1983; Siebert et
416 al. 1987; Belousov et al. 2004). These volcanoes provide examples of lateral collapse
417 initiated by magma intrusions and stress the importance that this represents for volcano

418 stability and hazard assessment. Instability can be related to the intrusion (dikes and
419 cryptodomes), as well as extrusion (summit domes) of fresh magma, and can trigger failures
420 through overloading and oversteepening, deformation, or mechanical- and temperature-
421 related changes in pore pressures (Elsworth & Voight 1996; Day 1996; McGuire 2003, Norini
422 and Acocella 2011; Samaniego et al. 2015). For example, the high eruption rates of silicic
423 domes and lava flows at Mount St. Augustine (USA) repeatedly produced an oversteepened,
424 unstable volcanic cone which then collapsed (Beget and Kienle 1992). At Ruapehu (New
425 Zealand) a paleomagnetic study (McClelland and Erwin 2003) revealed that a summit dome
426 could have played some contributory part in the destabilization of the edifice. High
427 temperatures (350°C) of some dacite blocks into the 9.5 Ka BP Murimotu formation
428 suggests that a dacite dome was active on Ruapehu immediately prior to the lateral
429 collapse. In Mexico, Macias et al. (2010) report that the late Pleistocene collapse of Tacaná
430 volcano was likely initiated by the extrusion of an andesitic lava dome that weakened the
431 structure of the cone. A recent contribution by Rincon et al. (2018) tried to explain, with
432 analog models, how volcanoes could be destabilized by magma intrusion. The authors noted
433 that a large and deep listric fault crossing the volcano can form when the magma body is
434 still located at the base of the cone. This explains why, in some cases, a volcanic edifice
435 could collapse even if the intrusion does not reach shallower levels. If any trigger induces
436 the slope failure at this stage, no juvenile material will be involved in the collapse. Rincon et
437 al. (2018) also noted that, when the intrusion reaches shallower levels, an elongated
438 subsidence forms at the summit of the cone and a bulge at the middle flank develops. The
439 same deformation was noted at Mount St. Helens before its collapse (Lipman et al. 1981)
440 and described also in other analogue experiments (Donnadieu and Merle, 1998). The
441 intrusion of a cryptodome (Figure 5) into the upper part of a volcanic edifice
442
443 Figure 5
444
445 decreases its stability due to many different factors, for instance lower shear strength of the
446 magmatic body and associated weakening structures, shallow seismicity on the flank caused
447 by edifice fracturing in response to intrusion, outward-dipping normal faults bounding a
448 summit graben, hydrothermal alteration of large portions of the edifice, and bulging (i.e.
449 increase in steepness) of the destabilized flank (Donnadieu et al. 2001). Elsworth and Voight

(1996) have drawn attention to the potential role of magmatic intrusions in triggering structural failure as a consequence of their raising pore fluid pressures by means of mechanical or thermal straining (thermal expansion) of the rock-fluid medium and/or hydrothermal fluid circulation. The thermal expansion can develop large uplift forces beneath a potentially unstable block (Elsworth and Voight 1995). The magma has a gas-rich phase at depth. This, coupled with magma degassing at shallower levels, could lead to excess upward-propagating pore pressures (Thomas et al. 2004). In addition, dehydration (boiling) of active hydrothermal systems during magma emplacement can lead to considerably elevated pore pressures (Reid 2004). Once a volcanic system has reached a critical state, collapse may be initiated by any trigger or simply occur because the factor of safety is reduced sufficiently. At Shiveluch volcano, the cause of the destabilization was the ascent of a batch of viscous, water-rich magma to shallow levels (Belousov et al. 1999). The failure occurred before magma intruded into the edifice suggesting that the trigger mechanism was not magma-associated. A more likely destabilizing mechanism could have been related to the increase of pore pressure in the edifice due to pressurized gas released from the ascending magma (Belousov et al. 1999). Evidences from fumarolic gases in the thermal springs at La Soufrière of Guadeloupe volcano (Lesser Antilles) suggest that the current activity is the result of a new magma intrusion which was progressively emplaced at shallow depth in the last decades (Villemant et al. 2014). The assessment of potential hazards associated with the evolution of the current unrest must consider the implications of recurrent intrusions and further pressurization of the hydrothermal system. The role of hydrothermal pressurization, linked with magma intrusion, on the basal friction along low-strength layers within the upper part of the edifice must be evaluated with regards to slope collapses (Borselli et al. 2011; Villemant et al. 2014).

### 2.5 Past and present climate implications

Climate can influence volcanic activity and plays an important role in the stability of a volcanic edifice. Heavy rains or hurricanes, for example, can promote massive landsliding over large areas. During the passage of Hurricane Mitch above Central America in 1998, heavy rains promoted a lateral collapse of Casita volcano (Nicaragua), killing 2,500 people (Kerle and van Wyk de Vries 2001; Scott et al. 2005). The source volume of the landslide (~200,000 $m^3$) was comparatively small to other giant volcanic collapse-related mass flows.

482 However, the landslide entrained older deposits and organic material during the flow,
483 transforming into a devastating debris avalanche (Kerle and van Wyk de Vries 2001) and
484 subsequently into a debris flow (Scott et al. 2005). It is common worldwide that debris
485 avalanches of Casita-size occur every few years (McGuire 1996; Kerle and van Wyk de Vries
486 2001). Climatic hazards rapidly affect widespread areas contributing to volcanic instability.
487 Heavy rains during wet seasons and glacier retreat have become more prominent over the
488 last several decades due to changing climatic conditions as a result of global warming (Capra
489 2006; Roberti et al. 2020 - this volume). Recent examples in periglacial environments of ice-
490 avalanches, rock avalanches, and a mix between both have been considered to be
491 increasing by these changing conditions (Huggel et al. 2007; Huggel et al. 2008; Tuffen 2010;
492 Kos et al., 2016; Coe et al. 2018; Hibert et al. 2019). The 2010 and other large landslides at
493 Mount Meager volcano (Canada), for example, resulted, in part, from glacier retreat and
494 erosion contributing to changes in stress of its already unstable slopes (Grämiger et al. 2017;
495 Roberti et al. 2020 - this volume). With current accelerated rates of glacial melting, glaciated
496 active volcanoes are at an increasing probability of generating landslides, from shallow
497 failures to debris flows to large-volume VDAs. Well-known paleo-climate records from the
498 last deglaciation show that melting of ice triggered a dramatic acceleration in volcanic
499 eruptions (Capra et al. 2015). However, major glaciations (and deglaciations) have been
500 considered not only as a triggering mechanism for large magmatic eruptions but also
501 inducing volcano instability (Capra et al. 2013). Ice-capped volcanoes are sensitive
502 environments to climatic changes, and large-scale glacial melting occurring at the end of the
503 Pleistocene, caused a significant increase in the incidence of large volcanic lateral collapse
504 and debris flows (Tormey 2010). Tormey (2010) reported that Planchon-Peteroa volcano
505 (Chile-Argentina border) had a large slope collapse that produced a highly mobile and
506 erosive debris avalanche 11,000 years BP, and other slope instabilities during the end of the
507 Pleistocene to early Holocene deglaciation. Capra (2006) suggested that most volcanic
508 lateral collapses of ice-capped volcanoes after the last main glacial peaks have been induced
509 by changing climatic conditions. The late Pleistocene and Holocene geological record
510 indicates that several volcanic slope collapses occurred in limited time spans at 1.4–1.3 ka
511 BP, at 1.0–0.9 ka BP, and at ~0.8 ka BP coinciding with several abrupt deglaciations at
512 different latitudes (Clapperton 1998; Capra 2006). Volcanic lateral collapse events in
513 periglacial environments are conditioned by different factors such as 1) shallow

514 hydrothermal alteration driven by snow and ice melting (Carrasco-Nuñez et al. 1993;
515 Waythomas et al. 1999; Roverato et al. 2011; Roverato and Capra 2013), 2) decreasing rock
516 mass-strength by abrasion and deformation due to glacier advancing (Capra et al. 2013), 3)
517 glacial plucking enhancing volcano weaknesses by exploiting preexisting fractures (Bennett
518 and Glasser, 2009) and 4) increasing pore pressures by high water circulation (Roberti et al.
519 2017). The high circulation of water in the collapsing mass could also strongly influence the
520 debris avalanche by transforming it into a debris flow-like rheology (Carrasco et al. 1993;
521 Capra et al. 2002; Roverato et al. 2011). Roverato et al. (2015) reported that at the time of
522 the Pungarehu collapse, during the Last Glacial Maximum, Taranaki volcano (New Zealand)
523 was not glaciated, but it did experience periglacial conditions. The snow/ice water-melting
524 coming from the glacier/snowfield or at least a high humid environment might suggest that
525 the pre-avalanche volcanic edifice was partially water-saturated. The increase in
526 precipitation arising from post-glacial warmer, wetter climatic conditions has been
527 considered possible trigger of catastrophic volcanic slope collapses (Capra 2006). This
528 ice/snow could have been an additional supply of water in the collapsed mass during the
529 Pungarehu event permitting the long runout of the avalanche (Roverato et al. 2015). Similar
530 conditions are reported, for example, by Alvarado et al. (2004) concerning volcanic slope
531 collapses in Costa Rica during the last glaciation, for the Teteltzingo collapse at Citlaltepetl
532 volcano (Carrasco-Nuñez et al. 1993) and for the Tonila event at Colima volcano (Roverato
533 et al. 2011). In light of the potential effects of climate change on landslide hazards, it is
534 crucial to monitor potential landslides locations and establish readily available methods for
535 early debris avalanche prediction (Huggel et al. 2008).
536

537 **3. The instability of volcanic islands**

538 Volcanic lateral collapses have been identified around volcanic islands worldwide
539 and their failure can trigger devastating tsunamis threatening coastal communities and
540 infrastructure (Karstens et al. 2019; Watt et al. 2020 - this volume). The term “volcanic
541 island” is a comprehensive term that includes the main endmembers: oceanic island and arc
542 island. The first ones are gently sloping oceanic shield volcanoes, such the Kilauea (Hawai’i,
543 USA) in the Pacific Ocean or the Piton de La Fournaise (Reunion Island, France) in the Indian
544 Ocean, usually associated with persistent flank movement (Poland et al., 2018). Oceanic
545 island volcanoes, especially in their active shield-building phase, are frequently affected by

546 large-scale lateral collapses (Moore and Fiske 1969; Elsworth and Day 1999). The arc
547 volcanic islands instead are usually steep-sided composite volcanoes such as Fogo (Cabo
548 Verde) in the Atlantic Ocean, Stromboli (Italy) in the Mediterranean Sea, or Augustine (USA)
549 in the Aleutian arc (Reid et al. 2010), associated with minimal ground deformation at the
550 flank-scale (González et al. 2010), sometimes with strong (volcaniclastic) material
551 remobilization (Di Traglia et al. 2018). Failures of volcanic islands include thin-skinned,
552 narrow collapse, and deep-seated instability events, removing much of an edifice and
553 depositing huge amounts (several $km^3$) of debris (Coombs et al., 2007; Montanaro et al.
554 2011). They represent the largest formations which can be created in a single geological
555 moment (Blahůt et al. 2018). In addition to the instability and triggering factors that affect
556 volcanoes in all geographical contexts (Voight and Elsworth 1997; Elsworth and Day 1999;
557 Reid et al. 2010), observing that >10 $km^3$-volume collapses occurred at the onset of glacial
558 to interglacial transitions, it suggested that rapid sea level rise enhanced changing of pore
559 pressure conditions, contributing to slope collapse (Quidelleur et al. 2008).
560 The classification of landslides on volcanic islands usually comprises two
561 endmembers: volcanic debris avalanches, thought to reflect a sudden single catastrophic
562 event, and slumps, thought to reflect progressive slope failure (Blahůt et al. 2018). Slumps
563 affects volcanic flanks with persistent motion and consequent flank deformation, as the
564 Hilina Slumps at Kilauea in Hawai'i (Okubo 2004) and the southeastern flank of the Pico
565 volcanic ridge in the Azores (Hildenbrand et al. 2012). Large VDADs have been observed on
566 the ocean floor surrounding the Hawaiian Islands (Iverson 1995; Morgan et al. 2003), the
567 Canarian Archipelago (Carracedo 1999; Hurlimann et al. 1999), Cape Verde (Elseworth and
568 Day 1999; Ramalho et al., 2015) and Azores (Hildebrand et al. 2018). Some of the debris
569 avalanches may develop by partial or complete collapse of a volcano slope already
570 oversteepened by a slump (Normark et al. 1993). Debris avalanches in arc volcanic islands
571 are typically smaller than those at ocean islands, but they are more frequent (Day et al.
572 2015). The VDADs around ocean islands and island arc volcanoes have similar slope
573 gradients in the deposition area, mobility and lithology (Karstens et al. 2019).
574 In historical times, tsunamigenic volcanic debris avalanches have caused many
575 casualties, two of the most devastating cases were: i) the 1792 Unzen–Mayuyama
576 megaslide (volume of $3.4\times10^8$ $m^3$ and the maximum depth was 400 m) that killed around
577 15,000 people, and ii) Ritter, Papua New Guinea, in 1888 (mobilized volume of about 4.2 x

578 $10^9$ $m^3$; Day et al. 2015 or 2.2-2.6 x $10^9$ $m^3$, Karstens et al. 2019). The slope collapse of Ritter
579 Island is the largest historically recorded landslide at a volcanic island (Cooke 1981; Day et
580 al. 2015; Karstens et al. 2019). The failure produced a headwall width of ~3 km and a fall in
581 vent elevation of ~1,500 m, reducing the 780 m high, 1.5-km-wide island to a small remnant
582 (Johnson, 1987). The landslide-induced tsunami affected islands out to ~600 km from Ritter,
583 killing hundreds of people and producing considerable damage (Cooke 1981; Day et al.
584 2015; Watt et al. 2019). Recent studies (Karstens et al. 2019; Watt et al. 2019) based on
585 high-resolution 2D and 3D seismic and bathymetric data, provided new insights into the
586 collapse sequence and landslide-induced tsunami generation. The collapse of Ritter
587 occurred in two phases: (1) the volcanic edifice was first affected by deep-seated gradual
588 spreading generating compressional deformation within the volcano and the adjacent
589 seafloor sediments; (2) the failure of about 2.4 $km^3$ of the island and the generation of a
590 highly energetic mass flow. This second phase is inferred to have been deposited up to 80
591 km from Ritter (Watt et al. 2019). The slide triggered an explosive phase that formed a
592 crater-like depression (Karstens et al. 2019).
593 More recently on 22 December 2018 the lateral collapse of the Anak Krakatau
594 occurred (Figure 6). The active volcanic island, situated within the Krakatau caldera in the
595 Sunda Strait between Java and Sumatra, experienced a slope collapse after a period of
596 intense volcanic activity (Williams et al. 2019). This event generated tsunami waves ranging
597 in height from 0.27 to 1.40 m, caused the deaths of 431 people, injured a further 7,200
598 people, and displaced 46,646 people (Williams et al. 2019).
599 A good example of a tsunamigenic landslide that occurred in recent times, and is
600 supported by many studies, is the one at Stromboli volcano during its 2002–2003 eruption
601 (Tinti et al., 2006).The volcanic island is located in the Tyrrhenian Sea off the southern coast
602 of Italy, and was affected by several mass-wasting events during its geological history,
603 mainly located in the northwest part of the volcano that produced a depression called
604 "Sciara del Fuoco" (Kokelaar and Romagnoli 1995; Tibaldi 2001). During the 2002–2003 flank
605 eruption, a submarine–subaerial landslide sequence (total volume of 25–30 x $10^6$ $m^3$,
606 Bonaccorso et al. 2003; Chiocci et al. 2008) generated two tsunamis. These tsunami waves
607 affected the coastline with a maximum run-up of 6–7 m at the Stromboli village (Tinti et al.,
608 2006) and were caused by two initial submarine rotational slides that affected the

underwater volcaniclastic apron down to a depth of 350 m (Chiocci et al. 2008), as well as by two second subaerial translational slides (Tommasi et al. 2005).

Figure 6

Geological and geotechnical studies (Tommasi et al. 2005; Chiocci et al. 2008; Boldini et al. 2009; Verrucci et al. 2019) suggest that the submarine and sub-aerial slides were caused by large deep-seated gravitational slope deformations (DSGSD) affecting the northern part of the Sciara del Fuoco, triggered by the injection of a lateral intrusion (Bonaccorso et al. 2003). The DSGSD developed under drained conditions, preventing the collapse of the entire block (Chiocci et al. 2008). Contrariwise, during its continuous displacement, excessive pore pressure was likely generated in the submarine volcaniclastic apron (undrained load condition), reducing the effective stresses down to values compatible with the static liquefaction of the material (Tommasi et al. 2005; Boldini et al. 2009).

Another volcano showing strong flank instability is Kilauea, on the Big Island of Hawai'i (USA). Kilauea is a persistently active volcano, partially overlapping the larger neighbour Mauna Loa, located in the middle of the Pacific Plate at the leading edge of a ~6,000-km-long chain of islands and seamounts. The south flank of Kilauea volcano, bracketed by two rift zones that extend from Kilauea's summit caldera, is creeping slowly seaward along a weak, low-angle décollement (Poland et al, 2017. Large scale slope collapse (volumes of 5,000 $km^3$) have been recognized. The Hilina Slump is the most notable of these features (Smith et al. 1999). Major rupture and offset on the southern flank have occurred along faults as recently as 1975, during the M7.2 Kalapana earthquake that struck the south coast of Hawai'i (Okubo 2004; Day et al. 2005). Kilauea's south flank experienced also transient aseismic displacements, as occurred in early November 2000, when an event of about 36 hours moved the flank at a maximum slip velocity of about 6 cm per day (Cervelli et al. 2002). The last transient flank motion occurred on early May 2018 that coincided with the lateral propagation of a dike along the East Rift Zone. The flank slip triggered a moment magnitude (Mw) 7.2 earthquake, producing ~5 meters of fault slip (Chen et al. 2019).

Other examples of failures of volcanic islands can be found in the Lesser Antilles arc, where 52 volcanic flank-collapse events are recognized, including the active volcanoes of Montserrat, Dominica, Martinique, and St. Lucia (Deplus et al. 2001; Boudon et al. 2013).

Large-scale debris avalanche deposits (10-20 $km^3$) lying on the seafloor around the islands, implying that relatively small volcanic islands, as Montserrat, can be affected by repeated large-volume landslides that deposit very large volcaniclastic material into the surrounding basins (Lebas et al. 2011). The largest deposits are related to collapses which include large sectors of the islands, both subaerial and submarine. However, it must be considered that even smaller subaerial landslides, associated with the collapse of lava domes, such as one that occurred on 26 December 1997 (the so-called "Boxing day" collapse; Voight et al. 2002), are extremely dangerous. At Soufrière Hills Volcano on Montserrat, a phase of dome growth started in the 1995. The collapse produced a $\sim 50 \times 10^6$ $m^3$ volcanic debris avalanche, and depressurized the interior of the lava dome, which exploded to generate a violent pyroclastic density current (Voight et al. 2002).

At Réunion Island spreading and avalanching developed in two different sectors (Le Friant et al. 2011). In particular, Réunion island is a 7,000 m-high volcanic complex with a large submarine part and two emerging volcanoes (Piton des Neiges and Piton de la Fournaise; Lénat et al. 1990; Lebas et al. 2018). Investigations by Le Friant et al. (2011) revealed that slow flank deformation is likely one of the main processes acting on the submarine flanks of Piton des Neiges, causing the continuous flank erosion by landslides, and producing turbidity flows (Bachèlery et al. 2003; Le Friant et al. 2011). Conversely, Piton de la Fournaise volcano collapsed several times in the same seaward direction, generating several voluminous debris avalanches that flowed down the submarine flanks. Le Friant et al. (2011) suggested that the difference in behaviour between the two volcanoes is likely related to the volcano basement. Piton des Neiges was built on marine sediments, promoting radial spreading, whereas Piton de la Fournaise was emplaced on the flank of a pre-existing edifice, favouring repeated collapses.

## 4- Discussion

Several contributing factors can affect the stability of volcanoes. These factors create the conditions that set the volcanic edifice to “ready to collapse”. According to classifications proposed by previous authors (Gorshkov, 1965; Moriya 1980; Siebert et al. 1987) three main failure categories exist: Bezymianny, Bandai, and Unzen/Ontake types. The difference between them is mainly based on the presence of a magmatic or phreatic explosive activity (Bezymianny and Bandai) or an earthquake as the trigger (Unzen/Ontake). The Bezymianny-

673 type collapse takes its name from the event that occurred in 1957 at Bezymianny Volcano
674 (Kamchatka), which was mainly related to a magmatic activity (Gorshkov, 1959;
675 Bogoyavlenskaya and Kirnasov 1981). This type of activity corresponds to the destabilization
676 of the volcanic edifice by magmatic intrusions and followed by magmatic eruptions. The
677 edifice undergoes strong deformation due to the emplacement of cryptodomes; the same
678 conditions that occurred at Mount St. Helens. The eruptive phase may contain highly
679 energetic lateral blasts (Belousov et al. 2004) with associated pyroclastic density currents.
680 The lateral blasts of Mount St. Helens and Bezymianny produced major pyroclastic density
681 currents that devastated areas of 500-600 $km^2$ around each of the volcanoes (Crandell and
682 Hoblitt 1986; Siebert et al. 1987). The Bezymianny activity is often followed by construction
683 of a lava dome or a new pyroclastic cone within the collapse scarp (Siebert et al. 1987; Leyrit
684 2000). In the case of Bezymianny volcano, the duration and magnitude of deformation, as
685 well as the presence of a flat lava dome in the crater prior to failure and magmatic eruptions
686 suggest that the intrusion was well developed. Other cryptodome-induced deformations
687 have been found at Showa-Shinzan and Usu-Shinzan (Katsui et al. 1985) of Usu volcano
688 (Minakami et al. 1951) in Japan. They did not culminate in a debris avalanche associated
689 with a paroxysmal eruption like at Mount St. Helens or Bezymianny (Donnadieu et al. 2001).
690 Bandai activity (Moriya 1980) refers to the explosion that occurred in 1888 at the Bandai-
691 San volcano (Japan). It is associated with phreatic explosions that favor the collapse of the
692 volcanic edifice without subsequent magmatic activity. It means that no juvenile material is
693 present neither within the debris avalanche deposit nor at the base or top of it. Massive
694 VDADs can also occur without related explosive eruptions, as at the Unzen volcano in 1792
695 or at Ontake volcano in 1984, where earthquake triggered the collapse. The potential of a
696 seismically-triggered volcanic edifice collapse to initiate a volcanic debris avalanche has
697 commonly been recognized (Voight and Elsworth, 1997; McGuire, 2003). Edifice collapse
698 and flank instability-derived deposits (VDADs) are now recognized as ubiquitous events
699 associated with active and growing volcanoes, yet the identification of the triggering
700 mechanisms is poorly correlated due to difficulties that lie in elucidating diagnostic
701 lithological and sedimentological features that record evidence of the trigger. Kataoka et al.
702 (2018) and Fairchild (1987) both highlight the importance of understanding the triggering
703 mechanisms of a landslide to then understand the emplacement mechanisms and resulting
704 hazard. Only in some cases such as Unzen-Mayuyama (1792), Bandai (1888), Bezymianny

(1956), Shiveluch (1964), Mount St. Helens (1980), and Ontake (1984) were observations of the events well-constrained enough that linkages could be made between initiation, trigger and flow through to emplacement and deposition. In the cases such as Unzen-Mayuyama (1792) and Ontake (1984) earthquakes were directly attributed to initiating the VDA. The 1792 Unzen-Mayuyama VDA is remembered as the trigger for a tsunami that impacted the Ariake Sea, killing ~14,500 people (Watanabe et al. 1993; Miyamoto 2010). Wang et al. (2019) states that from November 1791 to August 1792 earthquakes, eruptions and flows were recorded from various sites around Mt. Unzen. On the 21 May 1792 a magnitude 6.4 earthquake triggered a volcanic debris avalanche with an associated tsunami. Usami (1996) estimated that the earthquake which triggered a 3.4—4.8 x $10^8$ $m^3$ volcanic debris avalanche (Ui et al. 1986; Inoue 2000) was likely to have been of magnitude = 6.4 ± 0.2. This was estimated based on record that more that 30% of buildings in the Shimabara area were destroyed and ground ruptures were recorded which requires seismic accelerations of 400 $cm/s^2$ or more (Sassa et al. 2014). Sassa et al. (2014) also reported that ground accelerations of between 370 to 507 $cm/s^2$ were required from an earthquake to trigger a landslide of large enough volume to generate a tsunami of the size recorded. Although the geological and volcanological relationship between other volcanoes of the Unzen volcanic complex and Mayuyama is difficult to discern, the Mayuyama volcano or lava dome is considered to be 5.1±1.5 ka old (Hoshizumi et al., 1999) with the last recorded coeval activity at Unzen being a block-and-ash-flow at 4.2±110 ka B.P. Therefore, eruptive activity or intrusion into the dome was not a contributing factor in triggering the debris avalanche sourced from older brittle and dacitic volcanic rock. Another well-known earthquake-triggered edifice collapse is Ontake type, defined from the 1984 events from Ontake-San volcano. On 14 September 1984 the southeast slope of Ontake-San collapsed producing a 32-36 x $10^6$ $m^3$ avalanche (Voight and Sousa 1994). The last previous eruptive event at this volcano was in 1979 and since then the volcano had been dormant with the 1984 debris avalanche event being triggered by a magnitude 6.8 earthquake centered at 9-10 km southeast (Endo et al. 1989). The source rock was highly saturated andesite with interbedded or intercalated pyroclasts (Endo et al. 1989). Earthquake activity in this region is strongly aligned with regional stress fields, yet Sano et al. (1998) suggest some relationship with deeper-seated magmatic processes. Whereas Voight and Sousa (1994) focused on modeling the flowing mass and constraining parameters that increase mobility, little attention was paid to modeling the

737 initiation of the collapsing mass or fragmentation of that mass from the dynamic loading of
738 the earthquake.
739 The eruption from Mount St. Helens in 1980 is probably one of the most well-
740 described and documented events prior to, during and post- a VDA. Lipman and Mullineaux
741 (1982) and Christiansen et al. (1981) provide the chronology of the event identifying that
742 the magnitude 5.1 seismic event (Glicken 1996) triggered a series of events that lead to a
743 VDA. Endo et al. (1981) also identified that the magnitude 5+ earthquake had a hypocenter
744 depth of 1.5 km. The series of events (with respect to the VDA) recorded from eyewitness
745 accounts progress from the earthquake with avalanching of rocks from crater walls through
746 to "quivering" of the flank, fracturing and then slope failure. From the analysis of photos, it
747 is estimated that there were 7-20 seconds between the earthquake and the initiation of the
748 collapse (Voight et al., 1981). It is important to note that seismicity increased from 20 March
749 with seismicity being magnitude 4 or less considered to be confined to 2.5 km depth or less.
750 Dzurisin (2018) noted that by 27 March 1980, magma had intruded the edifice with
751 associated deformation being recorded. Voight et al. (1981) further postulated that the
752 failure was due to several cumulative facts, including progressive strength-loss prior to slip,
753 seismicity and gravitational movements, and increased pore pressure within rock units.
754 How earthquakes change the physical properties of the volcanic rock mass is not
755 well defined yet. The complexity of a volcano structure including its lithological layering,
756 variability of rock strengths, constructional boundaries, faulting, water storage,
757 hydrothermal activity, and others make the task of applying simple geotechnical analysis
758 difficult let alone introducing seismicity into the equation. The mechanisms that cause a
759 lateral collapse are in general cumulative or inter-related (Voight and Elsworth 1997) and
760 therefore it is difficult to identify a single initiation mechanism or trigger to edifice collapse
761 which would in turn negate the previous oversimplification of the Bezymianny, Bandai, and
762 Unzen/Ontake type of classifications previously used. It thus requires a more
763 comprehensive classification of edifice collapse based on a range of pre-conditioning and
764 triggering factors.
765 Voight and Elsworth (1997) identified that while the inherent properties of volcanic
766 rocks and the structure of the volcanic edifice are factors that contribute to volcano
767 instability, the driving factors that lead to collapse are generally changes in shear stress on
768 the rock mass. An important associated factor that changes the shear stress is variation in

pore fluid pressure. In terms of seismicity, earthquake shaking can increase pore fluid pressure in a saturated material. Modelling or simulating these types of relationships and processes within a volcanic edifice is difficult in particular on large stratovolcanoes where rock layers are massive and varying in thickness and rock strength is juxtaposed in a multitude of positions related to the evolution of that edifice over hundred or even thousands of years. Geotechnical analyses of the volcanic edifices have been undertaken around the world with success in identifying inherent instabilities in a variety of volcano types (e.g. Zimbelman et al. 2004; Moon et al. 2005; del Porto et al. 2013; Apuani et al. 2013).

Deutschle (2013) provided a comprehensive study of examining a range of triggers that contribute to flank instabilities on Mt. Taranaki in New Zealand. This complex stratovolcano has evolved over ~150,000 years and undergone up to 14 collapse events and regrowth resulting in a structurally and lithologically complex edifice (Zernack et al. 2012). Numerous limit equilibrium and finite element simulations that involved investigating rock strength variability due to changes in basement and edifice conditions, edifice growth, and magmatic intrusion show that while weaker areas of unconsolidated pyroclastic material exist on the current cone, it is still, in general considered stable unless magmatic intrusion or significant seismic shaking (>0.3 g) occurs (Deutschle 2013). Della Pasqua et al. (2016) undertook a similar analysis to understand the hazards posed by VDAs in the Taranaki region and found that susceptibility to failure will increase when there is higher seismic loads on weak, stratified layers. Alloway et al. (2005) identified a number of faults that traverse the Mt. Taranaki edifice and reconstructed earthquakes of magnitude 6.7-7.2 with shaking intensities of magnitude >8 with a recurrence interval of 4 ka. Keefer (1984) suggests that rock and soil avalanches require strong shaking intensities of magnitude >7-8. It is conceivable that a number of Mt. Taranaki VDADs were initiated by ground shaking associated with movements on those faults, but no conclusive evidence is presented in the literature. Earthquakes triggering VDAs is well recorded and while the triggering effects of the ground shaking to induce collapse have been elucidated from landslide investigations through understanding the physical properties of soils and rock, the initiation of the mass that suddenly loses its stability and move downslope is not well constrained or modelled accurately for volcanic edifices.

As we can see, most of the information available in the literature regarding eruptions and earthquakes, and their role in sector collapses, arises from historical cases or is inferred by theoretical models and simulations. However, if we take a look at the statistics of real cases, there is not much pre-historic information available about the triggering mechanisms that promote a sector collapse. Dufresne et al. (2020 - this volume) reports that only 16% of VDADs in a new global database of 1001 events have a related triggering mechanism; most of them are associated with magmatic activities. It is obvious that it proves difficult to associate a volcanic collapse with a specific trigger. However, some information on factors and processes involved in past collapses is recorded in the resulting deposits. In Table 3, we summarize key features that could be useful for studying VDADs in the field by providing information on the state of the pre-collapse volcanic edifice and the processes that acted before or during a sector collapse.

Table 3

Efforts to couple lateral collapse models and flow models as proposed in Voight and Sousa (1994) need to be further developed. Being able to transfer those simulations and predictions into a hazard and risk analysis framework (e.g. Mead et al. 2018) to provide a more holistic analysis of the event is also required considering that much of the motivation for understanding volcanic debris avalanches arose from better understanding the hazardous events that occurred over the last 300 years.

## 5- Conclusions

Volcanic sector collapses can be prepared by a wide variety of destabilizing factors, which are followed by triggering elements that drive the collapse (Figure 7). Although we group these factors in distinctive sections, it is evident that most of them are inherently related. In fact, factors that prepare and trigger volcanic sector collapses are not simple but can be multiple and cumulative. Over-steepened slopes, magma intrusions, hydrothermal activity, climate fluctuations, deformation of the basement, eruptions, earthquakes, are just a list of elements that could promote a volcanic collapse. Although it is necessary to identify the differences between those factors that define the degree of instability from those mechanisms that trigger the collapse, it is also important to define those factors that, in

combination, could lead to different catastrophic scenarios. Indeed, the mechanism that triggers a sector collapse could be independent of the causes that prepare its instability. But it is also true that multiple factors in consort could drastically enhance the power and magnitude of the collapse event and affect its runout.

Figure 7

The intrusion of a magma body (e.g. cryptodome) into a volcanic edifice, for example, has multiple consequences for the stability of the volcano. On one hand, the magma body deforms the edifice structure and, if the magma reaches the surface, its products could overload the volcanic flanks (destabilizing factor). On the other hand, the hydrothermal fluids associated with the magma body could promote all those processes of rock leaching and dissolution that weaken the volcanic material. If the intrusion of a magma body, linked with an earthquake or volcanic tremors, could be considered a factor that induce a volcanic collapse (trigger), clay mineral formation and migration due to the presence of magmatic fluids is an important element both for the loss of rock strength (destabilizing factor) as well as for the increase of impermeability that promote fluids and water (e.g. meteoric) storage. Once the collapse occurred, the presence of fluids and water, and the clay content as well, can play a fundamental role in the transport and mobility of the avalanche body, enhancing its mobility and transforming the moving mass into a cohesive lahar. Thus, considering all the endogenous and exogenous factors, a volcanic sector collapse and debris avalanche motion depend on an intricate system of factors that promote volcano instability, trigger the collapse, and enhance the avalanche mobility. It is therefore important to understand all the antecedent factors and triggers of volcano instability since that knowledge can provide critical precursory information that can directly inform hazard warnings.

**Acknowledgments**

We acknowledge Marc-André Brideau and Lucia Capra reviewers for their important suggestions and corrections that helped to notably improve the manuscript.

## References


Alloway B, McComb P, Neall V, Vucetich C, Gibb J, Sherburn S, Stirling M (2005) Stratigraphy, age, and correlation of voluminous debris-avalanche events from an ancestral Egmont Volcano: implications for coastal plain construction and regional hazard assessment. J Roy Soc New Zealand 35(1-2): 229-267

Alvarado GE, Veg E, Chaves J, Vasquez M (2004) Los grandes deslizamientos (volcánicos y no-volcánicos) de tipo debris avalanche en Costa Rica. Rev Geo de Am Centr 30:83-99

Andrade SD, van Wyk de Vries B (2010) Structural analysis of the early stages of catastrophic stratovolcano flank-collapse using analogue models. Bull Vulcanol 72:771-789

Apuani T, Corazzato C, Merri A, Tibaldi A (2013) Understanding Etna flank instability through numerical models. J Vol Geotherm Res 251: 112-126

Bachèlery P, Robineau B, Courteaud M, Savin C (2003) Debris avalanches on the western flank of Piton des Neiges shield volcano (Reunion Island). Bull Soc Géo de France 174(2): 125-140

Bahar I, Girod M (1983) Controle Structural Du Volcanisme Indonésie (Sumatra, Java-Bali); Application et Critique de La Methode de Nakamura." Bull Soc Géo de France XXV 7: 609-14

Begét JE, Kienle J (1992) Cyclic formation of debris avalanches at Mt. St. Augustine volcano, Alaska. Nature 356:701-704

Belousov A, Belousova M, Voight B (1999) Multiple edifice failures, debris avalanches and associated eruptions in the Holocene history of Shiveluch volcano, Kamchatka, Russia. Bull Volcanol 61(5):324-342

Belousov A, Voight B, Belousova M (2004) Directed blasts and blast-generated pyroclastic density currents: a comparison of the Bezymianny 1956, Mount St Helens 1980, and Soufrière Hills, Montserrat 1997 eruptions and deposits. Bull Volcanol 69:701-740

Bennett MR, Glasser NF (2009) Glacial Geology. Ice Sheets and Landforms. Wiley- Blackwell 385

Blahůt J, Klimeš J, Rowberry M, Kusák M (2018) Database of giant landslides on volcanic islands—first results from the Atlantic Ocean. Landslides 15(4): 823-827

Bogoyavlenskaya GE, Kirsanov IT (1981) Twenty-five years of activity of Bezymianny Volcano Vulkanologiya i Seismologiya 2:3-13

Boldini D, Wang F, Sassa K, Tommasi P (2009) Application of large-scale ring shear tests to the analysis of tsunamigenic landslides at the Stromboli volcano, Italy. Landslides 6(3): 231-240

Bonaccorso A, Calvari S, Garfì G, Lodato L, Patanè D (2003) Dynamics of the December 2002 flank failure and tsunami at Stromboli volcano inferred by volcanological and geophysical observations. Geo Res Letters 30(18): 1941.

Bonforte A, Guglielmino F, Coltelli M, Ferretti A, Puglisi G (2011) Structural assessment of Mount Etna volcano from Permanent Scatterers analysis. Geoch, Geophy, Geosys 12(2): Q02002.

Bonforte A, Guglielmino F, Puglisi G (2019) Large dyke intrusion and small eruption: The December 24, 2018 Mt. Etna eruption imaged by Sentinel-1 data. Terra Nova 31 (4): 405-412

Borgia A, Delaney PT, Denlinger RP (2002) Spreading Volcanoes. Annu Rev Earth Planet Sci 2000 28:539-70

Borgia A, Ferrari L, Pasquarè G (1992) Importance of gravitational spreading in the tectonic and volcanic evolution of Mount Etna. Nature 357:231-235

Borselli L, Capra L, Sarocchi D, De la Cruz-Reyna S (2011) Flank collapse scenario at Volcan de Colima, Mexico: a relative instability analysis. J Vol Geotherm Res 208:51-65

Boudon, G., Villemant, B., Le Friant, A., Paterne, M., & Cortijo, E. (2013). Role of large flank-collapse events on magma evolution of volcanoes. Insights from the Lesser Antilles Arc. J Vol Geotherm Res 263: 224-237

Capra (2006) Abrupt climatic changes as triggering mechanism of massive volcanic collapses. J Vol Geotherm Res 155:329-333

Capra L, Bernal JP, Carrasco-Nuñez G, Roverato M (2013) Climatic fluctuations as a significant contributing factor for volcanic collapses. Evidence from Mexico during the Late Pleistocene.

Glob and Plan Change 100:194-203
Capra L, Macias JL, Scott KM, Abrams M, Garduño-Monroy VH (2002) Debris avalanche and debris flow transformed from collapses in the Trans-Mexican Volcanic Belt, Mexico - behavior, and implication for hazard assessment. J Vol Geotherm Res 113:81-110
Capra L, Roverato M, Groppelli G, Caballero L, Sulpizio R, Norini G (2015) Glacier melting during lava dome growth at Nevado de Toluca volcano (Mexico): Evidences of a major threat before main eruptive phases at ice-caped volcanoes. J Vol Geotherm Res 294:1-10
Carracedo JC (1994) The Canary Islands : An Example of Structural Control on the Growth of Large Oceanic-Island Volcanoes. J Vol Geotherm Res 60: 225-41
Carracedo JC (1999) Growth, structure, instability and collapse of Canarian volcanoes and comparisons with Hawaiian volcanoes. J Vol Geotherm Res 94(1-4): 1-19
Carrasco-Núñez G, Díaz-Castellón R, Siebert L, Hubbard R, Sheridan MF, Rodríguez SR (2006). Multiple edifice-collapse events in the Eastern Mexican Volcanic Belt: The role of sloping substrate and implications for hazard assessment. J Volcanol Geotherm Res 158:151–176
Carrasco-Núñez G, Vallance JW, Rose WI (1993) A voluminous avalanche-induced lahar from Citlaltépetl volcano, Mexico: implications for hazard assessment. J Volcanol Geotherm Res 59(1-2):35-46
Cecchi E, van Wyk de Vries B, Lavest JM (2004) Flank spreading and collapse of weak-cored volcanoes. Bull Volcanol 67(1):72-91
Cervelli P, Segall P, Johnson K, Lisowski M, Miklius A (2002) Sudden aseismic fault slip on the south flank of Kilauea volcano. Nature 415(6875): 1014
Chen K, Smith JD, Avouac JP, Liu Z, Song YT, Gualandi A (2019) Triggering of the Mw 7.2 Hawaii earthquake of May 4, 2018 by a dike intrusion. Geoph Res Lett 46(5): 2503-2510
Chiocci FL, Romagnoli C, Tommasi P, Bosman A (2008) The Stromboli 2002 tsunamigenic submarine slide: characteristics and possible failure mechanisms. Journal of Geophysical Research: S Earth 113(B10): B10102.
Christiansen RL, Peterson DW, Lipman PW, Mullineaux DR (1981) Chronology of the 1980 eruptive activity. US Geol. Surv. Prof. Pap 1250: 17-30
Clapperton CM (1998) Late Quaternary glacier fluctuations in the Andes: testing the synchrony of global change. In: Owen LA (Ed.), Mountain Glaciation. Quaternary Proceedings, 6. John Wiley & Sons, Chichester, 65-73.
Clavero JE, Sparks RSJ, Huppert HE (2002) Geological constraints on the emplacement mechanism of the Parinacota avalanche, northern Chile. Bull Volcanol 64:40-54
Coe JA, Bessette-Kirton EK, Geertsema M (2018) Increasing rock-avalanche size and mobility in Glacier Bay National Park and Preserve, Alaska detected from 1984 to 2016 Landsat imagery. Landslides 15: 393
Cooke RJ (1981) Eruptive history of the volcano at Ritter Island. Geol Surv Papua New Guinea Mem, 10: 115-123
Coombs ML, White SM, Scholl DW (2007) Massive edifice failure at Aleutian arc volcanoes. Earth and Plan Scie Lett 256(3-4): 403-418
Crandell DR, Hoblitt RP (2006) Lateral blasts at Mount St. Helens and hazard zonation. Bull Volcanol 48:27-37Day SJ (1996) Hydrothermal pore fluid pressure and the stability of porous, permeable volcanoes. In: McGuire, W.J., Neuberg, J., Jones, A. (Eds), Volcano Instability on the Earth and Terrestrial Planets. Geol Soc London Spec Publ 110:77-93
Day SJ, Llanes P, Silver E, Hoffmann G, Ward S, Driscoll N (2015) Submarine landslide deposits of the historical lateral collapse of Ritter Island, Papua New Guinea. Marine and Petroleum Geology 67: 419-438
Day SJ, Watts P, Grilli ST, Kirby JT (2005) Mechanical models of the 1975 Kalapana, Hawaii earthquake and tsunami. Marine Geology 215(1-2): 59-92
Delaney PT, Pollard DD, Ziony JI, McKee EH (1986) Field Relations between dikes and joints: Emplacement processes and paleostress analysis. Journal of Geophysical Research 91(B5): 4920

969 Delcamp A, van Wyk de Vries B, James MR (2008) The influence of the edifice slope and substrata on
970 volcano spreading. J Vol Geotherm Res 177:925-943
971 Delmelle P, Bernard A (2015) The Remarkable Chemistry of Sulfur in Hyper-Acid Crater Lakes: A
972 Scientific Tribute to Bokuichiro Takano and Minoru Kusakabe, in Rouwet D, Christenson B, Tassi
973 F, Vandemeulebrouck J (Eds) Volcanic Lakes, Advances in Volcanology, Springer
974 del Potro R, Hürlimann M, Pinkerton H (2013) Modelling flank instabilities on stratovolcanoes:
975 parameter sensitivity and stability analyses of Teide, Tenerife. J Vol Geotherm Res 256: 50-60
976 della Pasqua F, Massey CI, McSaveney M, Townsend D (2016). Preliminary assessment of some flank-
977 failure scenarios for Mount Taranaki and recommendations for future assessment of the risk
978 from such hazards, GNS Science Report 2015/54: 48
979 Deplus C, Le Friant A, Boudon G, Komorowski JC, Villemant B, Harford C, Cheminée JL (2001)
980 Submarine evidence for large-scale debris avalanches in the Lesser Antilles Arc. Earth and Plan
981 Sci Lett 192(2): 145-157
982 Deutschle OK (2013) Characterisation of geotechnical units on Mount Taranaki and Influence on
983 Edifice Stability (Masters dissertation, University of Auckland).
984 Dufresne A, Siebert L, Bernard B (2020) Distribution and geometric parameters of volcanic debris
985 avalanche deposits, in Roverato M, Dufresne A, Procter J (Eds), Volcanic Dedris Avalanches:
986 From Collapse to Hazard, Advances in Volcanology, Springer
987 Di Traglia F, Nolesini T, Ciampalini A, Solari L, Frodella W, Bellotti F, Fumagalli A, De Rosa G, Casagli,
988 N (2018a) Tracking morphological changes and slope instability using spaceborne and ground-
989 based SAR data. Geomorphology 300:95-112
990 Donnadieu F, Merle O (1998) Experiments on the identation process during cryptodome intrusions:
991 New insights into Mount St. helens deformation. Geology 26:79-82
992 Donnadieu F, Merle O, Besson JC (2001) Volcanic edifice stability during cryptodome intrusion. Bull
993 Volcanol 63:61-72
994 Dzurisin D (2018) Mount St. Helens retrospective: Lessons learned since 1980 and remaining
995 challenges. Front in Earth Sci 6: 142
996 Endo ET, Malone SD, Noson LL, Weaver CS (1981) Locations, magnitudes, and statistics of the March
997 20–May 18 earthquake sequence. In The 1980 Eruptions of Mount St. Helens, Washington
998 (1250: 93-107). US Department of the Interior.
999 Endo K, Sumita M, Machida M, Furuichi M (1989) The 1984 collapse and debris avalanche deposits of
1000 Ontake Volcano, central Japan. In Volcanic Hazards (pp. 210-229). Springer, Berlin, Heidelberg.
1001 Elseworth D, Voight B (1995) Dike intrusion as a trigger for large earthquakes and the failure of
1002 volcano flanks. J Geo- phys Res 100(B4):6005-6024
1003 Elsworth D, Voight B (1996) Evaluation of volcano flank instability triggered by dyke intrusion.
1004 Geological Society, London, Special Publications 110 (1): 45-53
1005 Elsworth D, Day SJ (1999) Flank collapse triggered by intrusion: the Canarian and Cape Verde
1006 Archipelagoes. J Vol Geotherm Res 94(1-4): 323-340
1007 Fairchild LH (1987) The importance of lahar initiation processes. Debris flows/avalanches: process,
1008 recognition, and mitigation: Geo S of Am Rev in Eng Geo 7: 51-61
1009 Francis PW, Self S (1987) Collapsing volcanoes. Scientific American 256 (6): 90-99
1010 Francis PW, Wells GL (1988) Landsat Thematic Mapper observations of debris avalanche deposits in
1011 the Central Andes. Bull Volcanol 50: 258-78
1012 Francis PW (1994) Large volcanic debris avalanches in the central Andes. In: Proceedings of
1013 International Conference on Volcano Instability on the Earth and Other Planets. Geol Soc
1014 London.
1015 Frank D (1995) Surficial extent and conceptual model of hydrothermal system at Mount Rainier,
1016 Washington. J Vol Geotherm Res 65:51-80
1017 Frantz JD, Popp RK, Boctor NZ (1981) Mineral-solution equilibria - V. Solubilities of rock forming
1018 minerals in supercritical water. Geoch Cosm Acta 45:69-77
1019 Glicken H (1996) Rockslide-debris avalanche of May 18, 1980, Mount St. Helens volcano, Washington

(No. 96-677). US Geological Survey Open File Report.
González PJ, Tiampo KF, Camacho AG, Fernández J (2010) Shallow flank deformation at Cumbre Vieja volcano (Canary Islands): Implications on the stability of steep-sided volcano flanks at oceanic islands. Earth Plan Sci Lett 297(3-4):545-557
Gorshkov GS (1959) Gigantic eruption of the volcano Bezymianny. Bull Volcanol 21:77-109
Gorshkov GS, Bogoyavlenskaya GE (1965) Bezymianny volcano and peculiarities of its last eruption (1955–1963). Moscow, Nauka (in Russian)
Grämiger LM, Moore JR, Gischig VS, Ivy-Ochs S, Loew S (2017) Beyond debuttressing: mechanics of paraglacial rock slope damage during repeat glacial cycles. J Geophys Res Earth Surf 122(4):1004-1036
Hibert C, Michéa D, Provost F, Malet JP, Geertsema M (2019) Exploration of continuous seismic recordings with a machine learning approach to document 20 years of landslide activity in Alaska. Geophys J Intern 219:1138-1147
Hildenbrand A, Marques FO, Catalão J (2018) Large-scale mass wasting on small volcanic islands revealed by the study of Flores Island (Azores). Scientific reports 8(1):13898
Hildenbrand A, Marques FO, Catalão J, Catita CMS, Costa ACG (2012) Large-scale active slump of the southeastern flank of Pico Island, Azores. Geology 40(10):939-942
Hoshizumi H, Uto K, Watanabe K (1999) Geology and eruptive history of Unzen volcano, Shimabara peninsula, Kyushu, SW Japan. J Vol Geotherm Res 89(1-4):81-94
Huggel C, Caplan-Auerbach J, Wessels R (2008) Recent extreme avalanches: triggered by climate change? Eos 89(47):469-470
Huggel C, Caplan-Auerbach J, Waythomas CF, Wessels RL (2007) Monitoring and modeling ice-rock avalanches from ice-capped volcanoes: A case study of frequent large avalanches on Iliamna Volcano, Alaska. J Vol Geotherm Res 168:114-136
Hürlimann M, Ledesma A, Martí J (1999) Conditions favouring catastrophic landslides on Tenerife (Canary Islands). Terra Nova 11(2-3): 106-111
Inoue K (2000) Shimabara-Shigatusaku Earthquake and topographic changes by Shimabara Catastrophe in 1792
Inokuchi (1988) Gigantic landslides and debris avalanches on volcanoes in Japan: case studies on Bandai, Chokai and Iwate Volcanoes. Rep Nat Res Center Disaster Prevention 41:163–275 (in Japanese with English abstract)
Iverson RM (1995) Can magma-injection and groundwater forces cause massive landslides on Hawaiian volcanoes? J Vol Geotherm Res 66(1-4):295-308
John DA, Sisson TW, Breit GN, Rye RO, Vallance JW (2008) Characteristics, extent and origin of hydrothermal alteration at Mount Rainier Volcano, Cascades Arc, USA: Implications for debris-flow hazards and mineral deposits. J Vol Geotherm Res 175:289-314
Johnson RW (1987) Large-scale volcanic cone collapse: the 1888 slope failure of Ritter volcano, and other examples from Papua New Guinea. Bull Vol 49(5):669-679
Karstens J, Berndt C, Urlaub M, Watt SF, Micallef A, Ray M, Klaucke I, Muff S, Klaeschen D, Kühn M, Roth T, Böttner C, Schramm B, Elger J, Brune S (2019) From gradual spreading to catastrophic collapse–Reconstruction of the 1888 Ritter Island volcanic sector collapse from high-resolution 3D seismic data. Earth Plan S Lett 517:1-13
Kataoka KS, Matsumoto T, Saito T, Kawashima K, Nagahashi Y, Iyobe T, Suzuki K (2018) Lahar characteristics as a function of triggering mechanism at a seasonally snow-clad volcano: contrasting lahars following the 2014 phreatic eruption of Ontake Volcano, Japan. Earth, Planets and Space 70(1): 113
Katsui Y, Komuro H, Uda T (1985) Development of faults and growth of Usu-Shinzan cryptodome in 1977–1982 at Usu volcano, north Japan. J Fac Sci Hokkaido Univ, Ser IV 21:339-362
Keefer DK (1984) Landslides caused by earthquakes. G S A Bull 95(4): 406-421
Kerle N, van Wyk de Vries B (2001) The 1998 debris avalanche at Casita volcano, Nicaragua - investigation of structural deformation as the cause of slope instability using remote sensing. J

Vol Geotherm Res 105(1-2):49-63
Kokelaar P, Romagnoli C (1995) Sector collapse, sedimentation and clast population evolution at an active island-arc volcano: Stromboli, Italy. Bull Volcan 57(4):240-262
Kos A, Amann F, Strozzi T, Delaloye R, von Ruette J, Springman S (2016) Contemporary glacier retreat triggers a rapid landslide response, Great Aletsch Glacier, Switzerland. Geophys Res Lett 43(24):12466-12474
Kuhn D (2002) Fold and thrust belt structures and strike-slip faulting at the SE margin of the Salar de Atacama basin, Chilean Andes. Tectonics 21:1026
Lagmay AMF, Valdivia W (2006) Regional stress influence on the opening direction of crater amphitheaters in Southeast Asian volcanoes. J Vol Geotherm Res 158 (1-2): 139-50
Lagmay AMF, van Wyk de Vries B, Kerle N, Pyle DM (2000) Volcano instability induced by strike-slip faulting. Bull Volc 62 (4-5): 331-46
Lebas E, Le Friant A, Boudon G, Watt SFL, Talling PJ, Feuillet N, Deplus C, Berndt C, Vardy ME (2011) Multiple widespread landslides during the long-term evolution of a volcanic island: Insights from high-resolution seismic data, Montserrat, Lesser Antilles. Geoch, Geophys, Geosyst 12(5): Q05006.
Lebas E, Le Friant A, Deplus C, de Voogd B (2018) Understanding the Evolution of an Oceanic Intraplate Volcano from Seismic Reflection Data: A New Model for La Réunion, Indian Ocean. Journal of Geophysical Research: Solid Earth 123(2):1035-1059
Le Friant A, Lebas E, Clément V, Boudon G, Deplus C, De Voogd B, Bachèlery P (2011) A new model for the evolution of La Réunion volcanic complex from complete marine geophysical surveys. Geophys Res Lett 38(9): L09312.
Lénat JF, Bachèlery P, Bonneville A, Galdéano A, Labazuy P, Rousset D, Vincent P (1990) Structure and morphology of the submarine flank of an active basaltic volcano: Piton de la Fournaise (Réunion Island, Indian Ocean). Oceanol. Acta 10:211-223
Leyrit H (2000) Flank collapse and debris avalanche deposits. In: Volcaniclastic Rocks, from Magmas to Sediments. Edited by H. Leyrit and C. Montenat 111-129
Lipman PW, Mullineaux DR, (eds) (1981) The 1980 Eruptions of Mount St Helens, Washington. U.S. Geological Survey, Professional Paper 1250. 844 pp.
Lipman PW, Moore JG, Swanson DA (1981) Bulging of the north flank before the May 18 eruption-Geodetic data, in Lipman PW, Mullineaux, DR (Eds), The 1980 eruptions of Mount St. Helens, Washington: U.S. Geological Survey Professional Paper 1250-143-155
Lopez DL, Williams SN (1993) Catastrophic volcanic collapse: Relation to hydrothermal processes. Science 260:1794-1795
Lundgren P, Casu F, Manzo M, Pepe A, Berardino P, Sansosti E, Lanari R (2004) Gravity and magma induced spreading of Mount Etna volcano revealed by satellite radar interferometry. Geophys Res Lett 31(4)
Macias JL, Arce JL, Garcia-Palomo A, Mora JC, Layer PW, Espindola JM (2010) Late-Pleistocene flank collapse triggered by dome growth at Tacaná volcano, México-Guatemala, and its relationship to the regional stress regime. Bull Volcanol 72:33-53
MacLeod N (1989) Sector-failure eruptions in Indonesian volcanoes. Geol Indonesia 12:563-601
McClelland E, Erwin PS (2003) Was a dacite dome implicated in the 9,500 B.P. collapse of Mt Ruapehu? A palaeomagnetic investigation. Bull Volc 65:294-305
McGuire WJ (1996) Volcano instability: a review of contemporary themes. Geo Soc, London, Special Publications 110(1):1-23
McGuire WJ (2003) Volcano instability and lateral collapse. Revista 1: 33-45
McGuire WJ (2006) Lateral collapse and tsunamigenic potential of marine volcanoes, in Troise C, De Natale G, Kilburn CRJ (eds), Mechanisms of Activity and Unrest at Large Calderas. Geo Soc, London, Special Publications 269:121-140.
Mead S, Bebbington M, Procter J (2018). Emulation of the relationship between hazard intensity and volcanic processes. In EGU General Assembly Conference Abstracts (Vol. 20, p. 11000).

Merle O, Borgia A (1996) Scaled experiments of volcanic spreading. J Geophys Res: Solid Earth 101(B6):13805-13817
Merle O, Lenat JF (2004) Hybrid collapse mechanism at Piton de la Fournaise volcano, Reunion Island, Indian Ocean. J Geophysic Res 108(B3):2166
Minakami T, Ishikawa T, Yagi K (1951) The 1944 eruption of volcano Usu in Hokkaido, Japan. Bull Volcanol 11:45-157
Miyamoto K (2010) Numerical simulation of landslide movement and Unzen-Mayuyama disaster in 1792, Japan. J Disast Res 5(3): 280-287
Montanaro C, Beget J, Marti J, Siebert L, Coombs M (2011) Volcano collapse along the Aleutian Ridge (western Aleutian Arc). Nat Haz & Earth Sys Scie 11(3)
Moon V, Bradshaw J, Smith R, de Lange W (2005) Geotechnical characterisation of stratocone crater wall sequences, White Island Volcano, New Zealand. Engineering geology, 81(2):146-178
Moore JG, Fiske RS (1969) Volcanic substructure inferred from dredge samples and ocean-bottom photographs, Hawaii. G S A Bulletin 80(7):1191-1202
Morgan JK, Moore GF, Clague DA (2003) Slope failure and volcanic spreading along the submarine south flank of Kilauea volcano, Hawaii. J Geophys Res: Solid Earth 108(B9)
Moriya I (1980) Bandaian Eruption and Landforms Associated with It: Collection of Articles in Memory of Retirement of Prof. K. Hishimura. Vol. 66. Tohoku University
Murray JB, van Wyk de Vries B, Pitty A, Sargent P, Woller L (2018) Gravitational sliding of the Mt. Etna massif along a sloping basement. Bull Volc 80:40
Nakamura K (1977) Volcanoes as possible indicators of tectonic stress orientation-Principle and proposal. J Vol Geotherm Res 2: 1-16
Norini G, Agliardi F, Crosta G, Groppelli G, Zuluaga MC (2019) Structure of the Colima Volcanic Complex: Origin and Behaviour of Active Fault Systems in the Edifice, in Varley N, Connor CB, Komorowski JC (eds) Volcanic de Colima, Active Volcanoes of the World, Springer
Norini G, Capra L, Groppelli G, Agliardi F, Pola A, Cortes A (2010) The structural architecture of the Colima Volcanic Complex. J Geophys Res - Solid Earth 115:B12209
Norini G, Acocella V (2011) Analogue modelling of flank instability at Mount Etna: understanding the driving factors. J Geophys Res - Solid Earth 116:B07206.
Norini G, Bustos E, Arnosio M, Baez W, Zuluaga MC, Roverato M (2020) Unusual volcanic instability and sector collapse configuration at Chimpa volcano, central Andes. J Volc Geoth Res 393:106808
Norini G, De Beni E, Andronico D, Polacci M, Burton M, Zucca F (2009) The 16 November 2006 flank collapse of the south-east crater at Mount Etna, Italy: Study of the deposit and hazard assessment. J Geophys Res – Solid Earth 114:B02204
Norini G, Capra L, Groppelli G, Lagmay AMF (2008) Quaternary sector collapses of Nevado de Toluca volcano (Mexico) as consequence of regional tectonics and volcanic evolution. Geosphere 4 (5):854-871
Norini G, Lagmay AMF (2005) Deformed symmetrical volcanoes. Geology 33-7:605-608.
Normark WR, Moore JG, Torresan ME (1993) Giant volcano-related landslides and the development of the Hawaiian Islands. Submarine landslides: selected studies in the US Exclusive economic zone. US Geol Surv Bull 2002:184-196
Okubo CH (2004) Rock mass strength and slope stability of the Hilina slump, Kīlauea volcano, Hawai'i. J Volc Geoth Res 138(1-2):43-76
Paguican EM, Wyk de Vries B, Lagmay AMF (2012) Volcano-tectonic controls and emplacement kinematics of the Iriga debris avalanches (Philippines). Bull Volc 74 (9): 2067-81
Poland MP, Peltier A, Bonforte A, Puglisi G (2018) The spectrum of persistent volcanic flank instability: A review and proposed framework based on Kīlauea, Piton de la Fournaise, and Etna. J Volc Geoth Res 339: 63-80
Quidelleur X, Hildenbrand A, Samper A (2008) Causal link between Quaternary paleoclimatic changes and volcanic islands evolution. Geophys Res Lett 35(2): L02303.

1173 Ramalho RS, Winckler G, Madeira J, Helffrich GR, Hipólito A, Quartau R, Adena K, Schaefer JM (2015)
1174 Hazard potential of volcanic flank collpases raised by new megatsunami evidence. Sci Adv
1175 1:e1500456
1176 Reid ME (2004) Massive collapse of volcano edifices triggered by hydrothermal pressurization.
1177 Geology 32(5):373-376
1178 Reid ME, Christian SB, Brien DL (2000) Gravitational stability of three-dimensional stratovolcano
1179 edifices. J Geophy Res - Solid Earth 105(B3):6043-6056
1180 Reid ME, Keith TE, Kayen RE, Iverson NR, Iverson RM, Brien DL (2010) Volcano collapse promoted by
1181 progressive strength reduction: new data from Mount St. Helens. Bull Volc 72(6):761-766
1182 Reid ME, Sisson TW, Brien DL (2001) Volcano collapse promoted by hydrothermal alteration and
1183 edifice shape, Mount Rainier, Washington. Geology 29(9):779-782
1184 Rincon M, Marquez A, Herrera R, Alonso-Torres A, Granja-Bruña JL, van Wyk de Vries B (2018)
1185 Contrasting catastrophic eruptions predicted by different intrusion and collapse scenarios.
1186 Scientific Reports 8:6178
1187 Roberti G, Ward B, van Wyk de Vries B, Friele P, Perotti L, Clague JJ, Giardino M (2017) Precursory
1188 slope distress prior to the 2010 Mount Meager landslide, British Columbia. Landslides 15:637
1189 Roberti G, Roberts NJ, Lit C (2020) Climatic influence on volcanic landslides, in Roverato M, Dufresne
1190 A, Procter J (Eds), Volcanic Dedris Avalanches: From Collapse to Hazard, Advances in
1191 Volcanology, Springer
1192 Rosas-Carbajal M, Komorowski JC, Nicollin F, Gibert D (2016) Volcano electrical tomography unveils
1193 edifice collapse hazard linked to hydrothermal system structure and dynamics. Scientific
1194 Reports 6: 29899
1195 Roverato M, Capra L (2013) Características microtexturales como indicadores del transporte y
1196 emplazamiento de dos depósitos de avalancha de escombros del volcán de Colima. Rev Mex
1197 Ciencias Geol 30:512-525
1198 Roverato M, Capra L, Sulpizio R, Norini G (2011) Stratigraphic reconstruction of two debris avalanche
1199 deposits at Colima Volcano (Mexico): insights into pre-failure conditions and climate influence.
1200 J Volcan Geoth Res 207:33-46
1201 Roverato M, Cronin S, Procter J, Capra L (2015) Textural features as indicators of debris avalanche
1202 transport and emplacement, Taranaki volcano. GSA Bull. 127: 3-18
1203 Samaniego P, Valderrama P, Mariño J, van Wyk de Vries B, Roche O, Manrique N, Chédeville C,
1204 Liorzou, C, Fidel L, Malnati J (2015) The historical (218 ± 14 aBP) explosive eruption of Tutupaca
1205 volcano (Southern Peru). Bull Volcanol 77:51
1206 Sano Y, Nishio Y, Sasaki S, Gamo T, Nagao K (1998) Helium and carbon isotope systematics at Ontake
1207 volcano, Japan. Journal of Geophysical Research: Solid Earth 103(B10): 23863-23873
1208 Sassa K, Dang K, He B, Takara K, Inoue K, Nagai O (2014) A new high-stress undrained ring-shear
1209 apparatus and its application to the 1792 Unzen–Mayuyama megaslide in Japan. Landslides
1210 11(5): 827-842
1211 Schaefer LN, Di Traglia F, Chaussard E, Lu Z, Nolesini T, Casagli N (2019) Monitoring volcano slope
1212 instability with Synthetic Aperture Radar: A review and new data from Pacaya (Guatemala) and
1213 Stromboli (Italy) volcanoes. Earth-Scie Rev 192:236-257
1214 Scott KM, Vallance JW (1995) Debris flow, debris avalanche, and flood hazards at and downstream
1215 from Mount Rainier, Washington. US Geological Survey Hydrologic Investigation Atlas, HA-729
1216 Scott KM, Vallance JW, Kerle N, Macías JL, Strauch W, Devoli G (2005) Catastrophic precipitation-
1217 triggered lahar at Casita volcano, Nicaragua: occurrence, bulking and transformation. Earth Surf
1218 Proc Landforms 30:59-79
1219 Scott KM, Vallance JW, Pringle PT (1995) Sedimentology, behavior and hazards of debris flows at
1220 Mount Rainier, Washington. U.S. Geol Surv Prof Pap 1547:56
1221 Shea T, van Wyk de Vries B (2010) Collapsing volcanoes: the sleeping giants' threat. Geology Today
1222 26(2):72-77
1223 Shea T, van Wyk de Vries B (2008) Structural analysis and analogue modeling of the kinematics and

dynamics of rockslide avalanches. Geosphere 4:657-686
Shea T, van Wyk de Vries B, Pilato M, (2008) Emplacement mechanisms of contrasting debris avalanches at Volcán Mombacho (Nicaragua), provided by structural and facies analysis. Bull Volc 70:899-921
Siebert L (1984) Large volcanic debris avalanches: Characteristics of source areas, deposits, and associated eruptions. J Volcan Geoth Res 22: 163-97
Siebert L, Alvarado GE, Vallance JW, van Wyk de Vries B (2006) Large-volume volcanic edifice failures in Central America and associated hazards. In: Rose WI, Bluth GJS, Carr MJ, Ewert JW, Patino LC, Vallance JW (eds) Volcanic Hazards in Central America. Geol Soc Am Spec Pap 412:1-26
Siebert L, Glicken H, Ui T (1987) Volcanic hazards from Bezymianny-and Bandai-type eruptions. Bull Volcan 49(1):435-459
Siebert L, Roverato M (2020) A Historical Perspective on Lateral Collapse and Debris Avalanches, in Roverato M, Dufresne A, Procter J (Eds), Volcanic Dedris Avalanches: From Collapse to Hazard, Advances in Volcanology, Springer
Smith JR, Malahoff A, Shor AN (1999) Submarine geology of the Hilina slump and morpho-structural evolution of Kilauea volcano, Hawaii. Journal of volcanology and geothermal research 94(1-4):59-88
Thomas ME, Petford N, Bromhead EN (2004) The effect of internal gas pressurization on volcanic edifice stability: evolution towards a critical state. Terra Nova 16:312-317
Tibaldi A (1995) Morphology of pyroclastic cones and tectonics. Journal of Geophysical Research 100 (B12): 24521-24535
Tibaldi A (1996) Mutual influence of dyking and collapses at Stromboli Volcano, Italy. Geol Soc, London, Special Publications 110: 55-63
Tibaldi A (2001) Multiple sector collapses at Stromboli volcano, Italy: how they work. Bull Volcan 63(2-3):112-125
Tibaldi A, Lagmay AMF, Ponomareva VV (2005) Articles effects of basement structural and stratigraphic heritages on volcano behaviour and implications for human activities ( the UNESCO / IUGS / IGCP Project 455 ). Episodes 28 (3): 158-70
Tinti S, Pagnoni G, Zaniboni F (2006) The landslides and tsunamis of the 30th of December 2002 in Stromboli analysed through numerical simulations. Bull Volcanol 68:462–479
Tommasi P, Baldi P, Chiocci FL, Coltelli M, Marsella M, Pompilio M, Romagnoli C (2005) The landslide sequence induced by the 2002 eruption at Stromboli volcano. In Landslides: Risk Analysis and Sustainable Disaster Management (251-258). Springer, Berlin, Heidelberg
Tormey D (2010) Managing the effects of accelerated glacial melting on volcanic collapse and debris flows: Planchon-Peteroa volcano, Southern Andes. Glob Plan Ch 74 (2), 82–90
Tuffen H (2010) How will melting of ice affect volcanic hazards in the twenty-first century? Phil Trans R Soc A 368:2535-2558
Ui T (1983) Volcanic dry avalanche deposits—identification and comparison with nonvolcanic debris stream deposits. J Volcan Geoth Res 18(1-4):135-150
Ui T, Yamamoto H, Suzuki-Kamata K (1986) Characterization of Debris Avalanche Deposits in Japan. J Volcan Geoth Res 29 (1-4): 231-43
Urlaub M, Petersen F, Gross F, Bonforte A, Puglisi G, Guglielmino F, Krastel S, Lange D, Kopp H (2018) Gravitational collapse of Mount Etna's southeastern flank. Science advances 4(10):eaat9700.
Usami T (1996) Materials for comprehensive list of destructive earthquakes in Japan, 416-1995. Revised and Enlarged Edition. University of Tokyo Press: Tokyo, Japan.
Valderrama P, Roche O, Samaniego P, van Wyk de Vries B, Bernard K, Mariño J (2016). Dynamic implications of ridges on a debris avalanche deposit at Tutupaca volcano (southern Peru). Bull Volcan 78:14
Villemant B, Komorowski JC, Dessert C, Michel A, Crispi O, Hammouya G, Beauducel F, De Chabalier JB (2014) Evidence for a new shallow magma intrusion at La Soufrière of Guadeloupe (Lesser Antilles). J Vol Geoth Res 285:247-277

Vallance JW, Scott KM (1997) The Osceola mudflow from Mount Rainier: sedimentology and hazard implication of a huge clay-rich debris flow. GSA Bull 109:143-163
Vallance JW, Siebert L, Rose WI, Girón JR, Banks NL (1995) Edifice collapse and related hazards in Guatemala. In: Ida Y and Voight B (eds), Models of magmatic processes and volcanic eruptions. J Volcanol Geotherm Res 66:337-345
Van Bemmelen RW (1949) The geology of Indonesia: The Hague, Government Printing Office, 732
van Wyk de Vries B (1998) Extension Induced by Volcanic Loading in Regional Strike-Slip Zones. Geology 26(11): 983-986.
van Wyk de Vries B, Davies T (2015) Landslides, debris avalanches, and volcanic gravitational deformation. In The Encyclopedia of Volcanoes (665-685). Academic Press.
Van Wyk de Vries B, Fancis PW (1997) Catastrophic collapse at stratovolcanoes induces by gradual volcano spreading. Nature 387:387-390
van Wyk de Vries B, Matela RJ (1998) Styles of volcano-induced deformation: numerical models of substratum flexure, spreading and extrusion. J Vol Geoth Res 81:1-18.
van Wyk de Vries B, Merle O (1996) The effect of volcanic constructs on rift fault patterns. Geology 24 (7): 643
van Wyk de Vries B, Kerle N, Petley D (2000) A sector-collapse forming at Casita volcano. Geology 28:167-170
van Wyk de Vries B, Self S, Francis PW, Keszthelyi L (2001) A gravitational spreading origin for the Socompa debris avalanche: J Vol Geoth Res 105:225-247
Verrucci L, Tommasi P, Boldini D, Graziani A, Rotonda T (2019) Modelling the instability phenomena on the NW flank of Stromboli Volcano (Italy) due to lateral dyke intrusion. J Vol Geoth Res 371:245-262
Vidal N, Merle O (2000) Reactivation of basement faults beneath Volcanoes: A new model of flank collapse. J Vol Geoth Res 99 (1-4): 9-26
Villemant B, Komorowski JC, dessert c, Michel A, Crispi O, Hammouya G, Beauducel F, DE Chabalier JB (2014) Evidence for a new shallow magma intrusion at La Soufrière of Guadeloupe (Lesser Antilles) Insights form long-term geochemical monitoring of halogen-rish hydrothermal fluids. J Vol Geoth Res 285:247-277
Voight B (2000) Structural stability of andesite volcanoes and lava domes. Philosophical Transactions of the Royal Society of London. Series A: Math, Physic Engin Sci 358(1770):1663-1703
Voight B, Elsworth D (1997) Failure of volcano slopes. Geotechnique, 47(1): 1-31
Voight B, Glicken H, Janda RJ, Douglass PM (1981) Catastrophic rockslide avalanche of May 18. In The 1980 Eruptions of Mount St. Helens, Washington (1250: 347-377). US Geol Surv Prof Pap
Voight B, Janda RJ, Glicken H, Douglass PM (1983) Nature and mechanics of the Mount St Helens rockslide-avalanche of 18 May 1980. Geotechnique 33:243-273
Voight B, Komorowski JC, Norton GE, Belousov AB, Belousova M, Boudon G, Young SR (2002) The 26 December (Boxing Day) 1997 sector collapse and debris avalanche at Soufriere Hills volcano, Montserrat. Geol Soc, London, Memoirs 21(1):363-407
Voight B, Sousa J (1994) Lessons from Ontake-san: a comparative analysis of debris avalanche dynamics. Engineering Geology 38(3-4): 261-297
Wang J, Ward SN, Xiao L (2019) Tsunami Squares modeling of landslide generated impulsive waves and its application to the 1792 Unzen-Mayuyama mega-slide in Japan. Engineering Geology 256: 121-137
Watanabe K, Hoshizumi H, Itaya T (1993) K-Ar Ages of Unzen Volcano in Kyushu, Japan: With Some Aspects of Geology of Mayu-Yama.
Watt SFL, Karstens J, Micallef A, Berndt C, Urlaub M, Ray M, Desai A, Sammartini M, Klaucke I, Böttner C, Day S, Downes H, Kühn M, Elger J (2019) From catastrophic collapse to multi-phase deposition: Flow transformation, seafloor interaction and triggered eruption following a volcanic-island landslide. Ear Plan Sci Lett 517:135-147
Watt SFL, Karstens J, Berndt C (2020) Volcanic-island lateral collapse and their submarine deposits, in

Roverato M, Dufresne A, Procter J (Eds), Volcanic Dedris Avalanches: From Collapse to Hazard, Advances in Volcanology, Springer
Waythomas CF, Miller TP, Begét JE (1999) Record of late Holocene debris avalanche and lahar formation at Iliamna Volcano, Alaska. Am Geophys Union Trans 80: F1140
Waythomas CF, Wallace KL (2002) Flank collapse at Mount Wrangell, Alaska, recorded by volcanic mass-flow deposits in the Copper River lowland. Canad J Earth Scie 39:1257-1279
Williams R, Rowley P, Garthwaite MC, (2019) Reconstructing the Anak Krakatau flank collapse that caused the December 2018 Indonesian tsunami. Geology 47(10):973-976
Wooller L, van Wyk de Vries B, Cecchi E, Rymer H (2009) Analogue Models of the Effect of Long-Term Basement Fault Movement on Volcanic Edifices. Bull Volc 71 (10): 1111-31
Wooller L, van Wyk de Vries B, Murray JB, Rymer H, Meyer S (2004) Volcano spreading controlled by dipping substrata. Geology 32(7):573-576
Zernack AV, Cronin SJ, Bebbington MS, Smith IEM, Price RC, Procter JN (2012) Forecasting catastrophic stratovolcano collapse, a model based on Mt. Taranaki, New Zealand. Geology 40:983-986
Zimbelman DR (1996) Hydrothermal alteration and its influence on volcanic hazards Mount Rainier, Washington, a case history: PhD Thesis, Univ. Colorado, Boulder
Zimbelman DR, Watters RJ, Firth IR, Breit GN, Carrasco-Nuñez G (2004) Stratovolcano stability assessment methods and results from Citlaltepetl, Mexico. Bull Volc 66:66-79

Figure captions:

Figure 1 (a) Model showing crater opening perpendicular to dike propagartion (Nakamura 1977). (b) Model off crater opening perpendicular to the strike of normal faults and σHmax (Francis and Self 1987). (c) Crater openings in Andean volcanoes (Francis and Wells 1988). (d) Crater opening at an acute angle to the underlying strike-slip fault (Lagmay et al. 2000).

Figure 2 Analogue experiment results by Wooller et al. 2009 showing the fault patterns created, areas of instability and the main control of the main geometrical parameters. Figures from Wooller et al., (2009).

Figure 3 Google Earth image showing the Colima Volcanic Complex formed by the youngest Fuego de Colima volcano grown into the Paleofuego volcano depression (dashed line). Both volcanoes are located on the southern flank of the older and inactive Nevado de Colima volcano.

Figure 4 Example of highly hydrothermally altered material in a VDAD at Nevado del Ruiz, Colombia. *Espeletia* plants for scale at the top of the cliff are ~1.5 m tall (*photo: Matteo Roverato*).

Figure 5 USGS photograph took by Peter Lipman on April 27, 1980, showing the impressive bulge on the northeastern flank of the Mount St. Helens volcano few days before its collapse.

Figure 6 Moderate resolution, SENTINEL-2 multispectral images of the Anak Krakatau A) before (1st November 2018; true colour) and B) after (2nd February 2019; true color) the lateral collapse occurred on 22nd December 2018. After the collapse, the intense explosive volcanic activity started to re-fill the collapse scar, producing a small coastal tuff ring.

Figure 7 Sketch representation of the instability factors that can destabilize a volcano and the triggering mechanisms, such as explosive activity and earthquakes, which promote a volcanic sector

collapse. The top right rectangle represents schematically how the hydrothermal activity affects a volcanic edifice, promoting leaching and dissolution of the rock, favoring the formation of voids and the migration and accumulation of clay minerals, and consequently, fluid storage and impermeability. This promotes loss of strength and shear reduction of the rock. See the text for more details.

Tables:

Table 1 References used in the present text regarding factors that lead to the instability of volcanic edifices and trigger a volcanic sector collapse. Note that some references are underlined because they do not refer directly to volcanic lateral collapse but are still relevant for understanding aspects of the processes promoting a volcanic edifice failure.

Table 2 Examples of volcanic debris avalanche deposits that display hydrothermal alteration

Table 3 Key features in a VDAD that could suggest what happened in the volcano edifice before and/or during the lateral collapse event

Table 1

| **Instability factors** | **References** |
|---|---|
| Basement tectonics and faults | Nakamura 1977; Moriya 1980; Bahar and Girod 1983; Siebert 1984; Delaney et al. 1986; Ui et al. 1986; Francis and Self 1987; Francis and Wells 1988; Carracedo 1994; Tibaldi 1995, 1996; Elsworth and Voight 1996; van Wyk de Vries and Merle 1996, 1998; Lagmay et al. 2000; Vidal and Merle 2000; Norini and Lagmay 2005; Tibaldi et al. 2005; Lagmay and Valdivia 2006; Norini et al. 2008; Wooller et al. 2009; Norini et al. 2010; Paguican et al. 2012; Norini et al. 2019; Norini et al. 2020 |
| Sloping substrate and gravitational spreading | van Bemmelen 1949; Borgia et al. 1992; Vallance et al. 1995; Merle and Borgia 1996; van Wyk de Vries and Francis 1997; Francis and Wells 1998; van Wyk de Vries and Matela 1998; Borgia et al. 2000; van Wyk de Vries et al. 2001; Deplus et al. 2001; Clavero et al. 2002; Kuhn 2002; Morgan et al. 2003; Lundgren et al. 2004; Wooler et al. 2004; Carrasco-Núñez et al. 2006; Siebert et al. 2006; Del Camp et al. 2008; Shea et al. 2008; Norini et al. 2009; Andrade and van Wyk de Vries 2010; Norini et al. 2010; Shea and van Wyk De Vrie 2010; Bonforte et al. 2011; Norini and Acocella 2011; Roverato et al. 2011; Paguican et al. 2012; Murray et al. 2018; Norini et al. 2019 |
| Hydrothermal alteration | Frantz et al. 1981; Siebert 1984; Carrasco--Núñez et al. 1993; Lopez and Williams 1993; Frank 1995; Scott et al. 1995; Day 1996; Kerle and Zimbelman 1996; Vallance and Scott 1997; Voight and Elsworth 1997; Van Wyk de Vrie et al. 2000; van Wyk de Vrie 2001; Reid et al. 2001; Waythomas and Wallace 2002; Merle et al. 2003; Reid 2004; Zimbelman et al. 2004; Alvarado et al. 2004; Cecchi et al. 2005; John et al. 2008; Shea et al. 2008; Borselli et al. 2011; Roverato et al. 2011; Delmelle et al. 2015; Rosas-Carbajal et al. 2016; Valderrama et al. 2016; Norini et al. 2020 |

| | |
|---|---|
| Dikes and magma intrusions | Gorshkov 1959; Gorshkov and Bogoyavkenskaya 1965; Lipman et al. 1981; Voight et al. 1983; Siebert et al. 1987; Beget and Kienle 1992; Elsworth and Voight 1995; Day 1996; Elsworth & Voight 1996; Donnadieu and Merle 1998; Belousov et al. 1999; Donnadieu et al. 2001; McClelland and Erwin 2003; McGuire 2003; Belousov et al. 2004; Reid 2004; Thomas et al. 2004; Macias et al. 2010; Borselli et al. 2011; Norini and Acocella 2011; Villemant et al. 2014; Samaniego et al. 2015; Rincon et al. 2018 |
| Past and present climate implications | Carrasco-Nuñez et al. 1993; McGuire 1996; Clapperton 1998; Waythomas and Begét 2000; Kerle and van Wyk de Vries 2001; Scott et al. 2005; Capra 2006; Huggel et al. 2007; Huggel et al. 2008; Bennett and Glasser 2009; Tormey 2010; Tuffen 2010; Roverato et al. 2011; Capra et al. 2013; Roverato and Capra 2013; Roverato et al. 2015; Kos et al. 2016; Grämiger et al. 2017; Roberti et al. 2017; Roberti et al. 2020 (this volume) |
| | |
| **Triggering mechanisms** | **References** |
| Explosive eruptions (Bezymianny/Bandai types) | Gorshkov 1959; Gorshkov 1962; Moriya 1980; Bogoyavlenskaya and Kirnasov 1981; Ui 1985; Siebert et al. 1987; Voight and Elsworth 1997; Leyrit 2000; Donnadieu et al. 2001, Belousov et al. 2004; Dzurisin 2018 |
| Earthquakes (Unzen/Ontake type) | Christiansen et al. 1981; Endo et al. 1981; Lipman and Mullineaux 1981; Voight et al. 1981; Keefer 1984; Ui et al. 1986; Fairchild 1987; Endo et al. 1989; Watanabe et al. 1993; Voight and Sousa 1994; Glicken 1996; Usami, 1996; Voight and Elsworth 1997; Hoshizumi et al. 1998; Sano et al. 1998; Inoue 2000; Donnadieu et al. 2001; McGuire 2003; Miyamoto 2010; Sassa et al. 2014; Della Pasqua et al. 2016; Kataoka et al. 2018; Wang et al. 2019 |

Table 2

| **Deposit** | **Volcano** | **Reference** |
|---|---|---|
| Teteltzingo VDAD | Citlaltepetl volcano, Mexico | Carrasco-Núñez et al. (1993) |
| 1998 VDAD | Casita volcano, Nicaragua | Kerle and van Wyk de Vries (2001) |
| Chetaslina mass-flow | Mount Wrangell, Alaska, USA | Waythomas and Wallace (2002) |
| Piton de la Fournaise VDAD | Reunion Island, France | Merle and Lenat (2003) |
| Fortuna VDAD | Miravalles volcano, Costa Rica | Alvarado et al. (2004) |
| El Crater VDAD | Mombacho volcano, Nicaragua | Shea et al. (2008) |
| Tonila VDAD | Colima volcano, Mexico | Roverato et al. (2011) |

| | | |
|---|---|---|
| Tutupaca VDAD | Tutupaca volcano, Peru | Valderrama et al. (2016) |
| Chimpa Unit | Chimpa volcano, Argentina | Norini et al. (2020) |

1404

1405

1406 Table 3

| Key features | | Pre/syn-collapse setting |
|---|---|---|
| Hydrothermal alteration | The VDAD displays:<br>- color stains in those reaches (e.g. proximal) where the volcaniclastic material is not mixed with other materials;<br>- homogeneous yellowish matrix in portions (e.g. medial/distal) where the material is partially or completely mixed;<br>- high clay content | The edifice was affected by hot fluid circulation favoring hydrothermal alteration responsible for the weakening of the strength of the rock and promoting instability of the volcano. |
| Water content | The VDAD is characterized by a water-saturated (or semi-saturated) aspect displaying facies with characteristics between debris-flow deposits (DFDs) and VDADs<br><br>- homogenous and partially cemented matrix- preservation of millimetric porosity<br><br>The VDAD is often associated to DFDs that lying directly on top of it | The edifice was affected by high water content due to different climatic conditions such as:<br>- high precipitation in tropical settings<br>- presence of snow and/or ice in boreal settings or at high altitudes in tropical settings<br><br>These factors contribute to the instability of the volcanic edifice and could also increase the area affected by a VDA through flow transformation into more mobile debris flows |
| Pyroclastic deposits | Pyroclastic deposits such as pyroclastic density current (PDC) or fall-out deposits lying directly in contact on top of the VDAD displaying sharp contacts | Pyroclastic material situated on top of the VDAD suggests that an eruption likely occurred after the collapse event as consequence of the depressurization of the magmatic system. The sharp contact between PDC and VDA deposits suggests that the VDA had already ceased to move when the PDC material emplaced. The magmatic event was likely not responsible for the collapse and other triggering mechanisms are involved. |

| | | |
|---|---|---|
| | PDC deposits such as directed blasts and/or blast-generated PDC deposits are "intimately" associated with the VDAD. Some characteristics are:<br>- the contact between PDC and VDA deposits is very irregular<br>- twisted clastic dikes of PDC material penetrate into the VDAD<br>- in distal reached PDC deposits are located below and above the VDAD<br><br>These features could be associates to the following section (juvenile material). | These characteristics indicate that the VDA was still moving when the PDC material started to emplace on the upper surfaces of the VDA. PDC deposits located below the VDAD in distal portions suggest that the kinetic energy of the PDC material was higher than the VDA and that it emplaced before the arrival of the collapsing mass. This section could be associates with the following one (juvenile material). |
| Juvenile material | Fresh fragments of volcanic material (lava fragments or other pyroclastic material) are immersed into the VDAD | It indicates that the collapse was associated to a magmatic event that triggered the collapse. Fresh lava fragments could indicate the presence of a summit dome or a shallow intrusion. Vesiculated juveniles are the product of the explosive character of the eruption. |

1407

1408

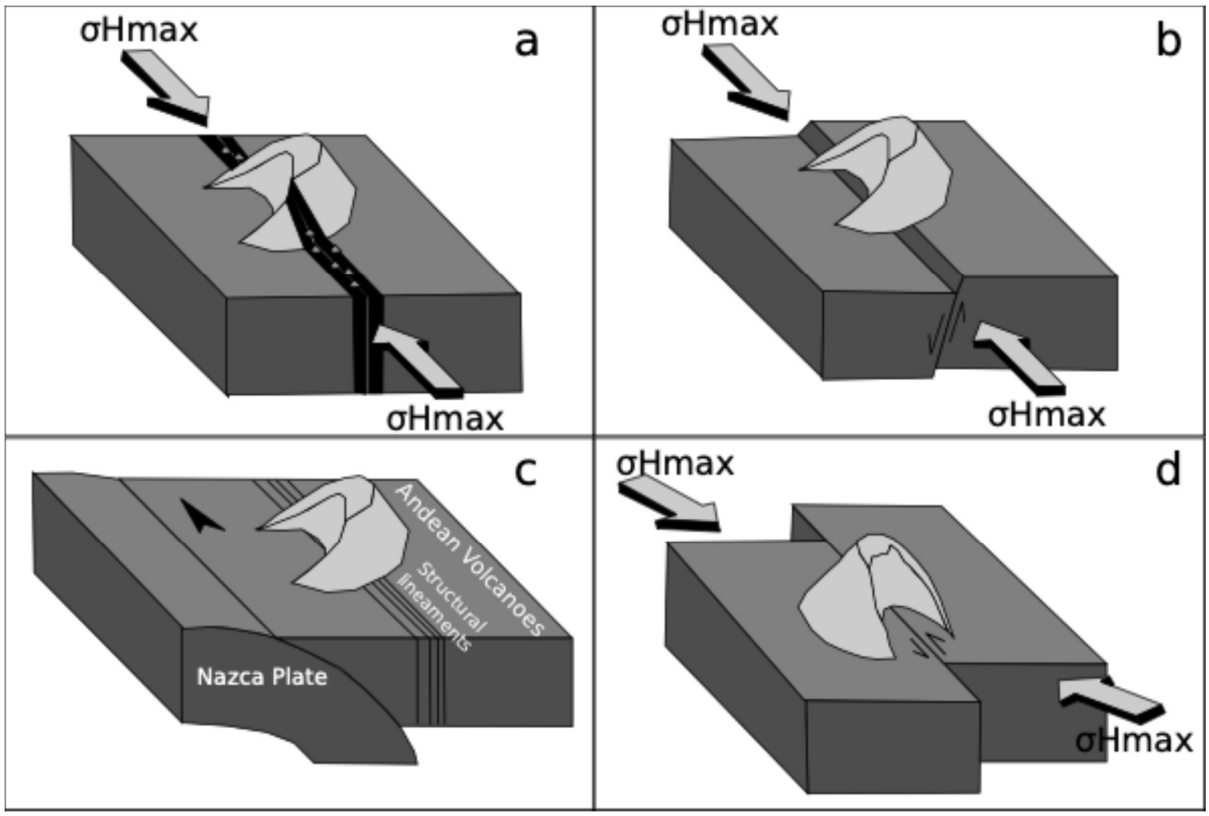
σHmax
a
σHmax
σHmax
b
σHmax
c
Andean Volcanoes
Structural lineaments
Nazca Plate
σHmax
d
σHmax

1409

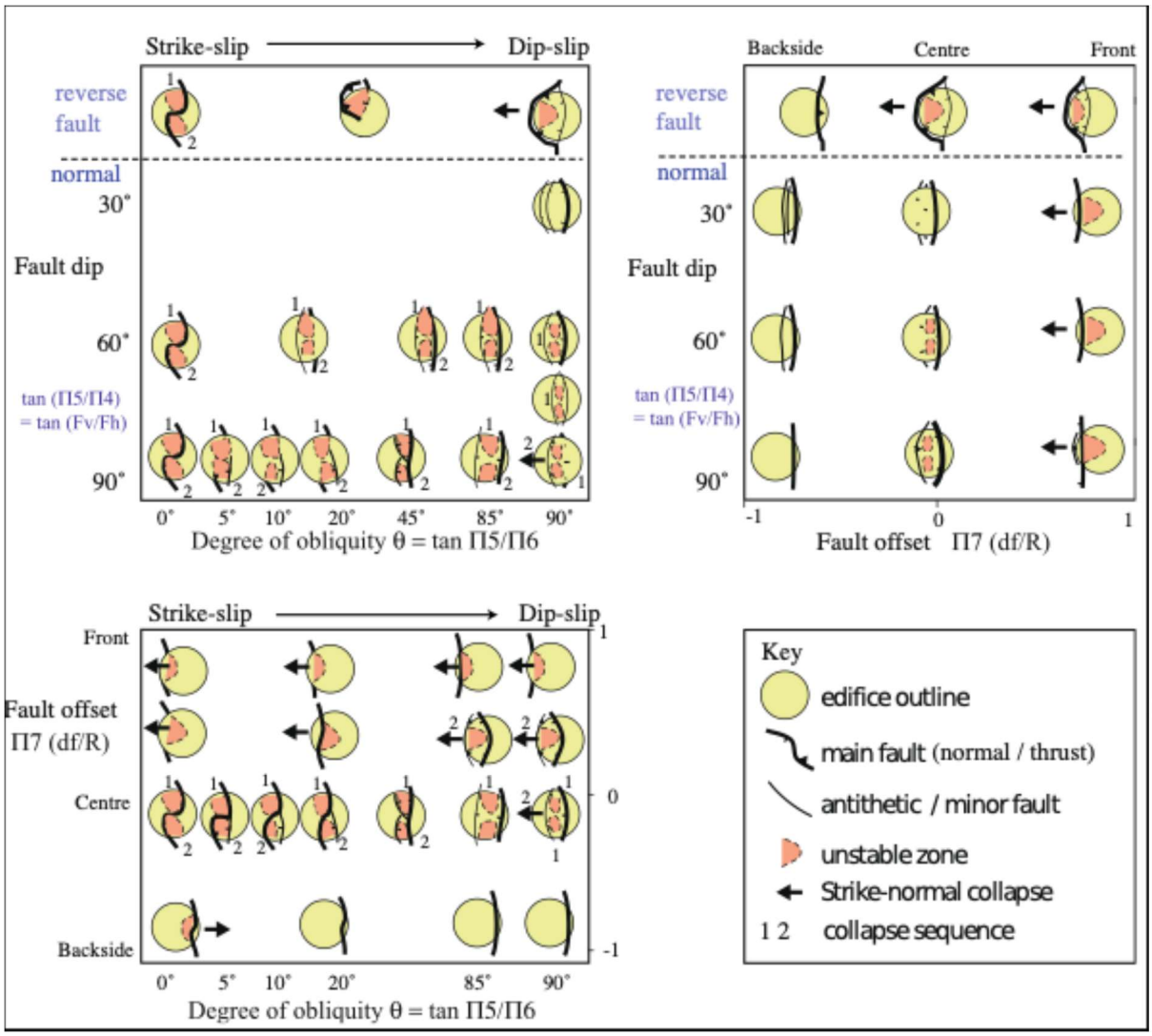
Strike-slip
Dip-slip
reverse fault
normal
30°
Fault dip
60°
tan (Π5/Π4) = tan (Fv/Fh)
90°
0° 5° 10° 20° 45° 85° 90°
Degree of obliquity θ = tan Π5/Π6
Backside
Centre
Front
-1 0 1
Fault offset Π7 (df/R)
Front
Fault offset Π7 (df/R)
Centre
Backside
1 0 -1
Key
edifice outline
main fault (normal / thrust)
antithetic / minor fault
unstable zone
Strike-normal collapse
1 2 collapse sequence

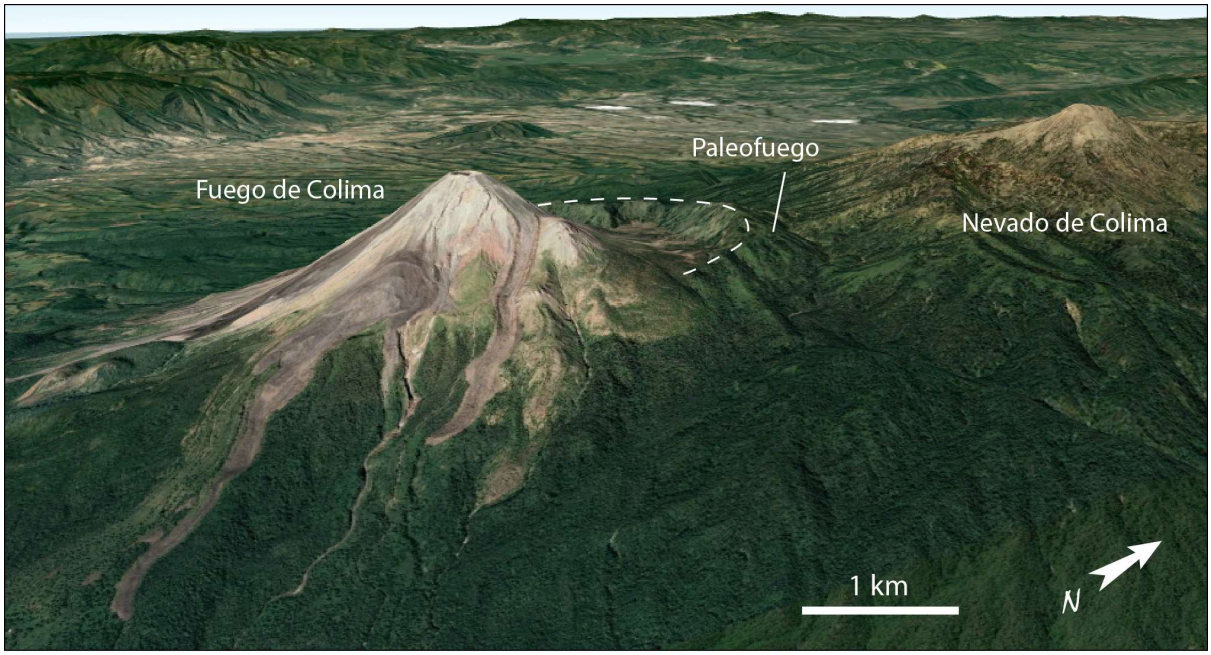
Fuego de Colima
Paleofuego
Nevado de Colima
1 km
N

1432

1433

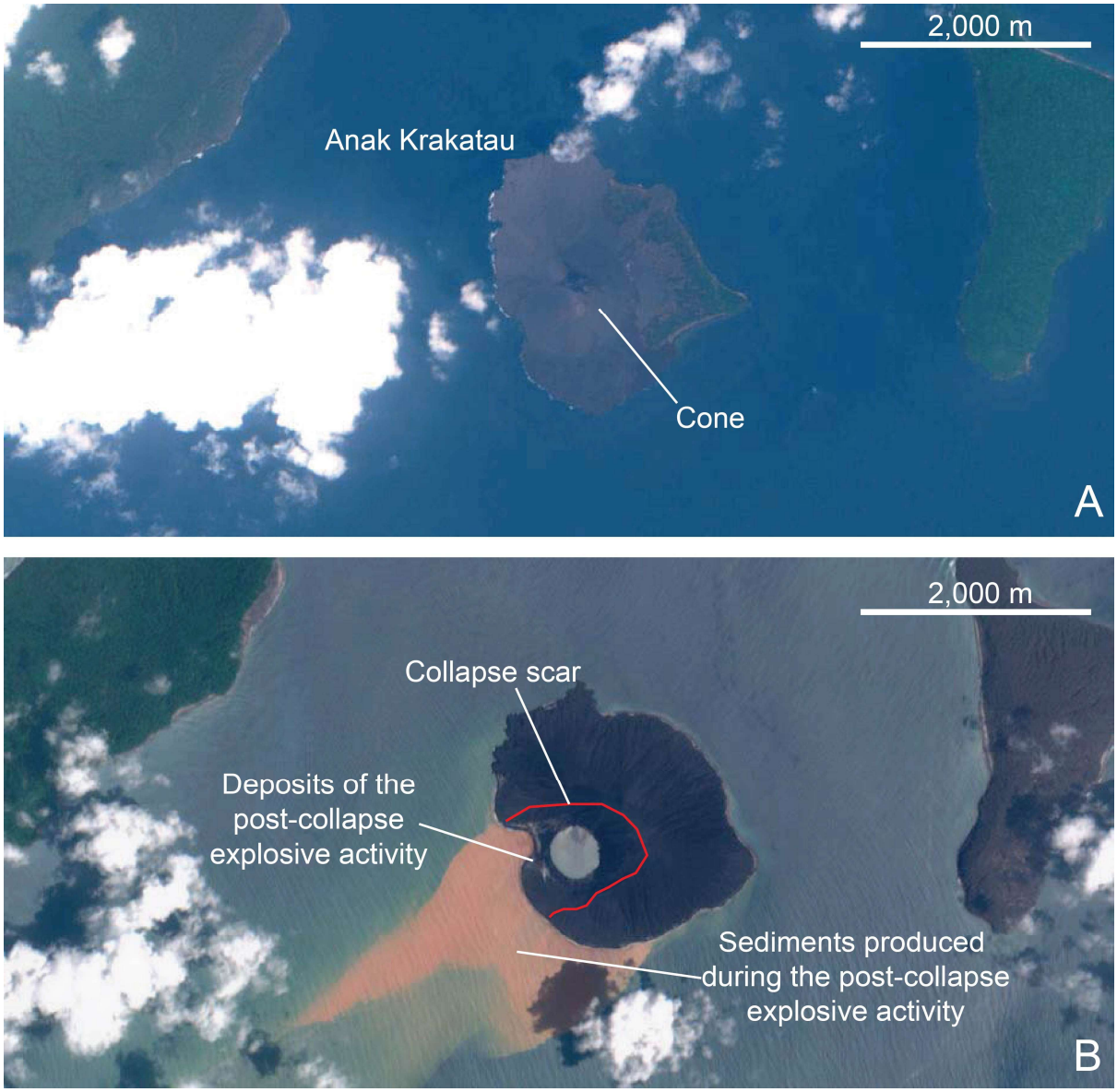
2,000 m
Anak Krakatau
Cone
A
2,000 m
Collapse scar
Deposits of the
post-collapse
explosive activity
Sediments produced
during the post-collapse
explosive activity
B

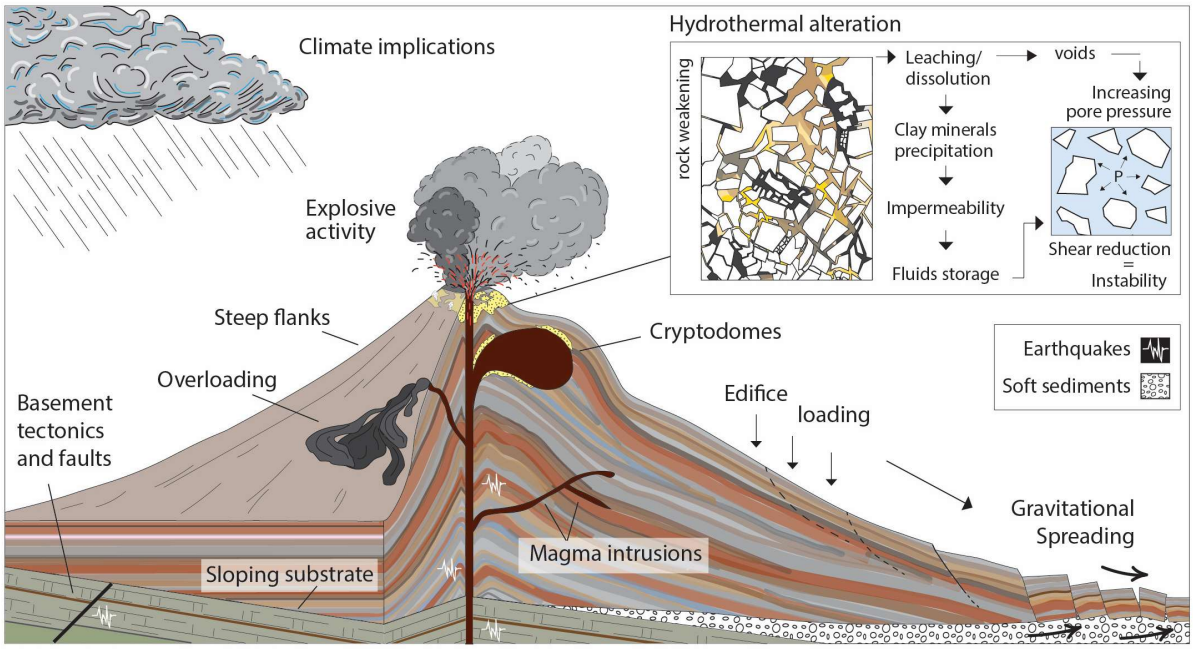
Climate implications
Hydrothermal alteration
rock weakening
Leaching/
dissolution
voids
Increasing
pore pressure
Clay minerals
precipitation
Impermeability
Fluids storage
P
Shear reduction
=
Instability
Explosive
activity
Steep flanks
Cryptodomes
Earthquakes
Soft sediments
Overloading
Basement
tectonics
and faults
Edifice
loading
Gravitational
Spreading
Magma intrusions
Sloping substrate

1453